

UNIVERSIDADE TÉCNICA DO ATLÂNTICO
INSTITUTO DE ENGENHARIA E CIÊNCIAS DO MAR

WEST AFRICAN SCIENCE SERVICE CENTRE ON CLIMATE CHANGE
AND ADAPTED LAND USE

Master's Thesis

**Behavioral and Foraging Pattern of Sharks
Across Oxygen Minimum Zones in The North
Atlantic Ocean:
Using Blue (*Prionace glauca*) and Shortfin Mako (*Isurus
oxyrinchus*) Sharks as Model Species**

TOLULOPE SAMUEL OYIKEKE

Master Research Program on Climate Change and Marine Sciences

São Vicente
2022



São Vicente
2022

UNIVERSIDADE TÉCNICA DO ATLÂNTICO
INSTITUTO DE ENGENHARIA E CIÊNCIAS DO MAR

WEST AFRICAN SCIENCE SERVICE CENTRE ON CLIMATE CHANGE
AND ADAPTED LAND USE

Master's Thesis

**Behavioral and Foraging Pattern of Sharks
Across Oxygen Minimum Zones in The North
Atlantic Ocean:
Using Blue (*Prionace glauca*) and Shortfin Mako (*Isurus
oxyrinchus*) Sharks as Model Species**

TOLULOPE SAMUEL OYIKEKE

Master Research Program on Climate Change and Marine Sciences

Supervisor | Dr. Nuno Queiroz
Co-supervisor | Dr. Marisa Vedor

São Vicente
2022

UNIVERSIDADE TÉCNICA DO ATLÂNTICO
INSTITUTO DE ENGENHARIA E CIÊNCIAS DO MAR

**WEST AFRICAN SCIENCE SERVICE CENTRE ON CLIMATE CHANGE
AND ADAPTED LAND USE**

Behavioral and Foraging Pattern of Sharks Across Oxygen Minimum Zones in The North Atlantic Ocean: Using Blue (*Prionace glauca*) and Shortfin Mako (*Isurus oxyrinchus*) Sharks as Model Species

Tolulope Samuel Oyikeke

Master's thesis presented to obtain the master's degree in Climate Change and Marine Sciences, by the Institute of Engineering and Marine Sciences, Atlantic Technical University in the framework of the West African Science Service Centre on Climate Change and Adapted Land Use

Supervisor



Dr. Nuno Queiroz
CIBIO-InBIO, University of
Porto

Co-supervisor

Marisa Graziela Cerqueira Vedor

Dr. Marisa Vedor
Biopolis/CIBIO-InBIO,
University of Porto

São Vicente
2022

UNIVERSIDADE TÉCNICA DO ATLÂNTICO
INSTITUTO DE ENGENHARIA E CIÊNCIAS DO MAR
WEST AFRICAN SCIENCE SERVICE CENTRE ON CLIMATE CHANGE
AND ADAPTED LAND USE

Behavioral and Foraging Pattern of Sharks Across Oxygen Minimum Zones in The North Atlantic Ocean: Using Blue (*Prionace glauca*) and Shortfin Mako (*Isurus oxyrinchus*) Sharks as Model Species

Tolulope Samuel Oyikeke

Panel defense

President

Examiner 1

Examiner 2

São Vicente
2022



Financial Support

The German Federal Ministry of Education and Research (BMBF) in the framework of the West African Science Service Centre on Climate Change and Adapted Land Use (WASCAL) through WASCAL Graduate Studies Programme in Climate Change and Marine Sciences at the Institute for Engineering and Marine Sciences, Atlantic Technical University, Cabo Verde.

Dedication

I dedicate this thesis to my parents for providing me with love, care, advice and encouragement during the completion of my thesis.

Acknowledgement

This study would not have been possible without the support and guidance of some individuals and institutions. First of all, I would like to express my sincere gratitude to my master's scholarship sponsor; the German Federal Ministry of Education and Research (BMBF), through the West African Science Service Centre on Climate Change and Adapted Land Use (WASCAL) Graduate Studies Program in Climate Change and Marine Sciences at the Institute for Engineering and Marine Sciences, Atlantic Technical University, Cabo Verde the opportunity to write a thesis in this program.

I want to express my sincere appreciation to the directress of the program, Dr Corrine Almeida, for her support from the beginning of the project work. In addition to my program directress, I would like to thank the rest of my thesis committee: Dr Antonio Pinto, Dr Estanislau Lima and Mrs Lizane Soares, for their encouragement, follow-ups, insightful comments and challenging questions.

The organization and completion of this project could not have been accomplished without the close guidance, patience, motivation, enthusiasm and mentoring of my thesis supervisor, Dr Nuno Queiroz and co-supervisor, Dr Marisa Vedor from the University of Porto. They indeed inspired this project and also created a favourable environment for the successful completion of this project. I also especially thank Dr Ivo Costa for his time and immense knowledge during my data analysis which helped me to reach most of my goals on time. My sincere thanks also go back to Dr Nuno Queiroz, who offered me the internship opportunity and experience with his research group while working on various exciting projects.

Finally, I would like to thank my special friend, Miss Jumoke Akinwoleola, for her emotional support and words of encouragement throughout the ups and downs of my Master's programme.

Resumo

Pensa-se que as alterações climáticas aumentam a expansão vertical e horizontal das zonas de oxigénio mínimo, quer comprimindo o habitat vertical dos peixes pelágicos, quer provocando uma mudança na sua distribuição. Contudo, não é claro como estes afectam o seu comportamento forrageiro e as interacções presas-predadores. Este estudo fornece informação de alta qualidade sobre o movimento, comportamento e preferências de habitat de tubarões azuis (*Prionace glauca*) e tubarões-anequim (*Isurus oxyrinchus*) para zonas de oxigénio mínimo, utilizando etiquetas de satélite (PSATs) e modelos ambientais, bem como dados *in situ* no norte central e leste do Atlântico tropical. A comparação entre os dados modelados de oxigénio e os dados *in situ* não mostrou diferença significativa ($p=0,07$) na ETA-OMZ. Em contraste, as concentrações de oxigénio de ambos os conjuntos de dados no Atlântico Norte e Sul mostraram diferenças significativas ($p=0,04$). A combinação de vários factores, que incluem o aquecimento dos oceanos e a desoxigenação oceânica associada às alterações climáticas, contribuiu para a compressão vertical dos habitats dos tubarões azuis e mako e aumentou a sua vulnerabilidade à pesca. Os resultados mostraram como a profundidade máxima de mergulho dos tubarões responde especificamente aos diferentes gradientes de oxigénio dissolvido. A ocupação espaço-temporal dos tubarões azuis e mako foi associada a frentes oceanográficas, forrageadoras e interacções predadoras ao longo da ZEE de Cabo Verde e do Sara Ocidental. Além disso, a ocupação do tubarão Mako do Sahara Ocidental foi atribuída a uma elevada concentração de clorofila -a que se sobrepõe a actividades de pesca com palangre pelágico de grande porte. Dado que o estatuto global destas espécies modelo continua a diminuir, é necessário implementar medidas de conservação e gestão offshore.

Palavras-chave: Alterações Climáticas, Zonas Mínimas de Oxigénio, Comportamento de Forragem, Oxigénio Dissolvido, Pesca

Abstract

Climate change is thought to increase the vertical and horizontal expansion of oxygen minimum zones, either compressing the vertical habitat of pelagic fish or causing a shift in their distribution. However, it is unclear how these affect their foraging behaviour and prey-predator interactions. This study provides high-quality information on the movement, behaviour, and habitat preferences of blue sharks (*Prionace glauca*) and shortfin mako sharks (*Isurus oxyrinchus*) to oxygen minimum zones using satellite tags (PSATs) and environmental models, as well as *in situ* data in the central north and eastern tropical Atlantic. The comparison between oxygen modelled and *in situ* data showed no significant difference ($p=0.07$) in the ETA-OMZ. In contrast, the oxygen concentrations of both datasets in the North and South Atlantic showed significant differences ($p=0.04$). The combination of various factors, which include ocean warming and ocean deoxygenation associated with climate change, has contributed to the vertical habitat compression of blue and mako sharks' habitats and increased their vulnerability to fishing. Results showed how the maximum diving depth of sharks responds specifically to different dissolved oxygen gradients. Spatiotemporal occupancy of blue and mako sharks was associated with oceanographic fronts, foraging and prey-predator interactions along Cape Verde's EEZ and Western Sahara. Additionally, the Mako shark's occupancy of Western Sahara has been attributed to a high concentration of chlorophyll-a that overlaps with high pelagic longline fishery activities. As the global status of these model species continues to decline, conservation and management measures offshore need to be implemented.

Keywords: Climate Change, Oxygen Minimum Zones, Foraging Behavior, Dissolved Oxygen, Fisheries

Abbreviations and Acronyms

CAN	Central North Atlantic
CMEMS	Copernicus Marine Environment Monitoring Service
EEZ	Exclusive Economic Zone
ETA	Eastern Tropical Atlantic
GLODAP	Global Ocean Data Analysis Project
IUCN	International Union for Conservation of Nature
JGOFS	Joint Global Ocean Flux Study
MDD	Maximum Dive Depth
OACES	Ocean-Atmosphere Carbon Exchange Study
OMZ	Oxygen Minimum Zones
P_{crit}	Critical PO ₂ describe the degree of hypoxia tolerance in fishes
PSAT(s)	Pop-up satellite archival tags
WOCE	World Ocean Circulation Experiment

General Index

Financial Support.....	i
Dedication.....	ii
Acknowledgement.....	iii
Resumo.....	iv
Abstract.....	v
Abbreviations and acronyms.....	vi
General Index.....	vii
List of Figures.....	x
List of Tables.....	xiii
1. Introduction.....	1
1.1 Background to the study.....	1
1.2 Problem Statement.....	2
1.3 Research Objectives.....	4
1.4 Research Hypothesis.....	5
1.5 Relevance and Importance of the Research.....	5
1.6 Structure of the Work.....	5
2. Literature Review.....	7
2.1 Oxygen Minimum Zones (OMZs).....	7
2.1.1 Variation in Depth of Oxygen Minimum Zones.....	9
2.1.2 Expansion of Oxygen Minimum Zones.....	9
2.1.3 Causes of Oxygen Minimum Zones Expansion.....	10
2.1.4 Oxygen Minimum Zones and Habitat Compression.....	12
2.1.5 Consequences of Oxygen Minimum Expansion.....	13

2.2 Behavioral and Physiological Adaptations of Fishes to Low Oxygen	14
2.2.1 Responses of Oxygen Minimum Zone Species to Hypoxic Conditions	14
2.2.2 Behavioural Adaptations	16
2.3 Study Preference of Blue and Shortfin Mako sharks	16
2.3.1 The Blue Shark (<i>Prionace glauca</i>).....	17
2.3.2 The Shortfin Mako shark (<i>Isurus oxyrinchus</i>).....	18
2.4 Past Studies.....	19
3. Materials and Methods	24
3.1 Study Area	24
3.2 Data Collection.....	25
3.2.1 Shark Data Collection.....	25
3.2.2 Environmental Data.....	28
3.2.3 Fishing Effort Geolocation	30
3.3 Method of Data Analysis.....	31
3.3.1 GLODAP and CMEMS Data Integration.....	31
3.3.2 Statistical Analysis	31
3.3.3 Environmental Integration of Oxygen with Shark Movement Data.....	33
3.3.4 Mapping Shark distribution and the Environment	34
3.3.5 Shark and Fishing Vessel Spatial overlap and effort.....	35
3.3.6 Ethical Consideration	35
4. Results	37
4.1 Result One: Comparison between CMEMS and GLODAP data	37
4.1.1 CMEMS vs GLODAP Oxygen concentrations.....	37
4.2 Result Two: Identification and Characterization of Shark Foraging and Habitat Use in OMZ.....	42
4.2.1 Habitat Use	42
4.2.1 Foraging and Environmental fields	43

4.3 Result Three: Hypoxia-Based Habitat Compression and Vulnerabilities to Fisheries.....	46
4.3.1 Oxygen Induced Habitat Compression and Shark behaviour.....	46
4.3.2 Shark’s Vulnerabilities to Fisheries.....	53
5. Discussion.....	55
6. Conclusion.....	59
References	61
Appendixes	70
Appendix 1	70

List of Figures

Figure 2. 1: Oceanic OMZs (A) CMEMS Global Modelled Integrated dissolved oxygen concentrations from 0 m to 200 m depth in the water column. (B) Visual interpolation of the mean in-situ acquired integrated oxygen concentration from 0 m to 200 m depth (GLODAP 2021)	8
Figure 2. 2: Microbial biogeochemical processes active in OMZs and the oxygenated ocean. Characteristic depth profile for dissolved oxygen in the eastern tropical North Atlantic (Beman et al., 2012; Gilly et al., 2013), indicating the depths of the euphotic zone (yellow), oxygen limited zone (OLZ; light gray), and OMZ (dark gray).....	8
Figure 2. 3: Dissolved oxygen and habitat changes in the eastern Atlantic. (A) Depth of 3.5 ml l ⁻¹ dissolved oxygen surface area (m) on January 1, 2010. (B) Average vertical change in 3.5 ml l ⁻¹ dissolved oxygen surface area 1960-2009 (m yr ⁻¹ : blue indentation). C) Change in dissolved oxygen (ml l ⁻¹ year ⁻¹) at depth of 3.5 ml l ⁻¹ surface in 2010. D(E), summed area of sorted grid points by depth of 3.5 ml l ⁻¹ dissolved oxygen content for the in B(D) and the corresponding average habitat loss relative to surface over the cumulative area due to the change in D(E). (Stramma et al., 2012)	13
Figure 2. 4: Blue Shark (<i>Prionace glauca</i>) (Marylou, 2020a)	18
Figure 2. 5: Shortfin Mako shark (<i>Isurus oxyrinchus</i>) (Ines Ferreira, 2020).....	19
Figure 3. 1: Map showing the spatial extent of the study area overlaid on oxygen concentration at 100 m depth.....	24
Figure 3. 2: North Atlantic-wide movements of (A) Blue and (B) Mako sharks in relation to the ETA dissolved oxygen at 100 m depth. Sharks were tracked PSATs (deployed in the western and central North Atlantic and above the ETA OMZ) superimposed on modeled dissolved oxygen concentrations (at 100 m).	26
Figure 3. 3: MiniPAT tag showing: (A) Argos antenna, (B) temperature sensor, (C) communications port with plug, (D) light sensor (1 of 2), (E) float, (F) release pin, (G) LED light, (H) wet/dry sensor, (I) ground plate, (J) light sensor (2 of 2), (K) pressure sensor (Source: Wildlife Computers, 2016, 2017).....	27
Figure 3. 4: Process of shark tagging PSAT rigged through the dorsal fin of a Mako shark from two different sides of the boat.....	28

Figure 3. 5: Map distribution of the complete tracks of sharks, study area and GLODAP data geolocation across the Atlantic Ocean.....	33
Figure 4. 1: Vertical gradient of oxygen concentration of CMEMS and GLODAP recorded in 2011	38
Figure 4. 2: Vertical gradient of oxygen concentration of CMEMS and GLODAP recorded in 2017	39
Figure 4. 3: Vertical gradient of oxygen concentration of CMEMS and GLODAP recorded in 2018	40
Figure 4. 4: Variation in oxygen concentrations between GLODAP and CMEMS in the (A) North/South Atlantic Ocean; (B) OMZs of ETA.	41
Figure 4. 5: Correlation test between GLODAP and CMEMS (A) North/South Atlantic Ocean (B) OMZs of ETA	41
Figure 4. 6: Kernel density of utilization distribution from pooled geolocation tracks over study period. (A) Number of blue shark (left) and Mako sharks (right) per grid cell (B) Days blue shark (left) and Mako shark (right) spent per grid cell (C) Mean days spent per grid cell	43
Figure 4. 7: Map of the study area in the North-east Atlantic. Three-year (2011, 2017, 2018) monthly average of dissolved oxygen at 100 m depth on the resident time (contour lines) of (A) Blue Sharks with residence time of 3 days (B) Mako sharks.with mean residence time of 28 days	44
Figure 4. 8: Map of the study area in the North-east Atlantic. Three-year (2011, 2017, 2018) monthly average of Chlorophyll a on the resident time (contour lines) of (A) Blue Sharks with residence time of 3 days (B) Mako sharks. With mean residence time of 28 days	45
Figure 4. 9: Map of the study area in the North-east Atlantic. Three-year (2011, 2017, 2018) monthly average of sea temperature at 100 m on the resident time (contour lines) of (A) Blue Sharks with residence time of 3 days (B) Mako sharks.with mean residence time of 28 days.....	46
Figure 4. 10: Dive response of blue sharks to oxygen concentration (A) Vertical movement of Blue sharks in relation to dissolved oxygen models. Daily maximum depth plots (black) for blue shark overlaid on GLODAP (red), CMEMS (yellow), and GLODAP-CMEMS (blue) DO concentration data at 100 m [see legend] (B) CMEMS DO concentration from the surface to 2000 m during shark movement (C) GLODAP DO concentration from the surface to 2000 m during shark	

movement. The dark grey area corresponds to where no data was available (D) CMEMS-GLODAP DO concentration from the surface to 2000 m during shark movement. 49

Figure 4. 11: Dive response of Mako sharks to oxygen concentration (A) Vertical movement of blue sharks in relation to dissolved oxygen models. Daily maximum depth plots (black) for blue shark overlaid on GLODAP (red), CMEMS (yellow), and GLODAP-CMEMS (blue) DO concentration data [see legend] (B) CMEMS DO concentration from the surface to 200 m during shark movement (C) GLODAP DO concentration from the surface to 200 m during shark movement (D) CMEMS-GLODAP DO concentration from the surface to 200 m during shark movement. 52

Figure 4. 12: Spatial distributions and overlap of sharks and longline fishing vessels. Distribution of the mean monthly overlap and the level of fishing effort (in days) that sharks were exposed to in overlapping areas for all species within $1^\circ \times 1^\circ$ grid cells (A) Percentage density of exposure of blue sharks in $1^\circ \times 1^\circ$ grid cells (B) Percentage density of exposure of blue sharks in $1^\circ \times 1^\circ$ grid cells..... 54

List of Tables

Table 3. 1: Summary of satellite tag deployments on blue and shortfin mako sharks in the North Atlantic including ID, track dates, and deployment locations decoded via satellite.....	25
Table 4. 1: Statistical summary of GLODAP vs CMEMS.....	42

1. Introduction

1.1 Background to the study

Dissolved oxygen (DO) is a crucial indicator of different biogeochemical and physical processes in the ocean, making it a key parameter for understanding the ocean's role in the climate system. Additionally, the distribution of dissolved oxygen in the world's oceans is regulated by air-sea interaction, ocean circulation, and oxygen uptake through photosynthesis (Bopp et al., 2002; Brandt et al., 2015; Levin, 2018).

The terms that have been used to describe the overall conditions of oxygen in the ocean are: anoxic, suboxic, and oxic (Karstensen et al., 2008). Several vital mobile macro-organisms are stressed or die under hypoxic conditions, i.e., when oxygen concentrations drop below ~ 60 to 120 mmol kg^{-1} (Paytan and McLaughlin, 2007). Hypoxia occurs at different oxygen concentrations among various species of microorganisms, so the threshold is not precise. Regions with dissolved oxygen concentrations below $60 \text{ } \mu\text{mol kg}^{-1}$ are termed hypoxia, while suboxia has dissolved oxygen less than $5 \text{ } \mu\text{mol kg}^{-1}$ (Deutsch et al., 2011; Craig, 2012). Anoxic regions have no dissolved oxygen. Currently, the mid-depth, oxygen-depleted layers called the oxygen minimum zone (OMZ) are suboxic in the eastern tropical Pacific and northern reaches of the tropical Indian Ocean and hypoxic in the tropical Atlantic.

OMZs have changed considerably over geological times and possibly altered the ocean carrying capacity of carbon and nitrogen significantly (Meissner et al., 2005). Permanent OMZs are present in all the world's ocean basins and occur where dissolved oxygen (DO) reaches low (hypoxic) levels of $<0.45\text{--}1.00 \text{ ml l}^{-1}$ in the depth range of $\sim 200\text{--}800 \text{ m}$ (Keeling et al., 2010; Gilly et al., 2013). Ocean deoxygenation has led to the horizontal and vertical expansion of OMZs with the prospect of profound impacts on marine biota, as long-term DO decline in OMZs is particularly acute (Stramma et al., 2008; Gilly et al., 2013; Breitburg et al., 2018). In conjunction with the weak vertical and lateral ventilation that characterizes the Eastern Tropical Atlantic (ETA), the oxygen consumption at the intermediate depths of the ocean leads to large OMZs (Al Azhar et al., 2017). Oxygen minimum zones (OMZs) are oxygen-poor regions of the ocean that are expanding due to the warming of the water column caused by global climate change (Wright et al., 2012). Large-scale climate change is causing the oceans to absorb more heat, resulting in less surface dissolved oxygen (reduced solubility) and increased

stratification of near-surface waters. At depths of 100 m and 700 m in the eastern tropical Pacific, north-central Atlantic and ETA are associated with OMZs (Johannes Karstensen et al., 2008) partly as a result of their proximity to the eastern boundary currents, which are some of the most biologically productive regions of the world's oceans as a consequence of the upwelling of nutrient-rich waters there.

According to Stramma et al. (2008), the expansion of OMZs in the world oceans has a major implication for biogeochemical cycles, in particular those of carbon and nitrogen, and might also have deleterious effects on the functionality and services of an ecosystem (Chan et al., 2008; Keeling et al., 2010). Model-based scenarios of the “future ocean” predict an overall dissolved oxygen decline and consequent expansion of OMZs under global warming conditions (Luyten et al., 1983; Gilly et al., 2013). Rosa and Seibel (2008) predicted that the synergy between ocean acidification, global warming, and expansion of OMZs would further reduce the habitat for large oceanic predators. The shoaling of the upper layers of the OMZs accompanies OMZ expansion, and the depletion of oxygen at shallower depths can adversely affect marine organisms through several direct and indirect mechanisms, including altering the microbial processes that produce essential nutrients and gases and consume them. Additionally, it can lead to changes in predator-prey dynamics and shifts in the abundance and accessibility of commercially fished species (Gilly et al., 2013).

The present study, therefore, aims to provide the first quality information on the movements, behaviour and habitat preferences of blue and shortfin mako sharks in the North Atlantic with respect to oxygen concentration and fishing effort (assessed using satellite AIS data). Two different oxygen datasets were used with the main objective of identifying regions of habitat compression to determine susceptibility to capture risk.

1.2 Problem Statement

Pelagic sharks are ecologically important oceanic top predators with somewhat high physiological demands for oxygen (Payne et al., 2016) that have been widely observed in the surface layers above OMZs (Vetter, 2008; Nasby-Lucas et al., 2009; Abascal et al., 2011; Queiroz et al., 2016; Queiroz et al., 2019; Sims, 2019). Oxygen loss in the ocean has major causes, and this includes eutrophication and deoxygenation caused by ocean warming, leading to reduced mixing of oxygen-rich waters near the surface with deeper waters (IUCN, 2019). Thus the question is whether the expanding volumes and

coverage of deoxygenated water such as OMZ have an adverse effect on the horizontal and vertical extent of these pelagic sharks to such extent that their habitat is compressed to a water depth of few hundreds of meters or their preys are somewhat more concentrated in the upper depth of the water column thereby increasing their vulnerabilities and exposing them to fish capture (Baum et al., 2003; Ferretti et al., 2010; Worm et al., 2013; Campana, 2016; ICCAT, 2017a; ICCAT, 2019).

Pelagic sharks are targeted every year by fishermen in long lines and with other methods on high seas that harvest these sharks in large amounts due to unsupervised or unregulated fisheries on international water where oversights are poor, which has led to overfishing and declining catch rates recorded for many of these pelagic shark species (ICCAT, 2019). Two of such pelagic sharks are the blue shark (*Prionace glauca*) and shortfin mako shark (*Isurus oxyrinchus*), which are two of the most heavily fished sharks in the world and are captured in great numbers either as a target or bycatch species of high-seas longliners (Stevens, 2000). Due to the estimated and inferred decline, together with the likely increase in fishing pressure and the life history of this species, it was recently listed as Vulnerable (IUCN 2009).

The ETA ocean OMZs serve as an appropriate system to study in this context because of the observed expansion of this OMZ that has been recorded over the last 50 years, with dissolved oxygen declines that are particularly intense compared to other OMZs (Stramma et al., 2008). This has continued over a long period (on more than decadal scales) but has variable upper and lower depth limits controlled by natural processes and cycles (Helly and Levin, 2004). However, this is about to change as recent expansion trends associated with climate change have been identified in several ETA-OMZs (Stramma et al., 2008; Keeling et al., 2010).

On a global scale, approximately 1,150,000 km² of the ocean is exposed to low oxygen concentrations < 0.7 mg O₂⁻¹ from OMZs (Helly and Levin, 2004). The specially adapted species that live in these hypoxic zones differ from the shallower species exposed to the seasonal or episodic hypoxia having much lower oxygen tolerance thresholds and morphological adaptations to maximise respiratory surface. (Levin, 2003). As hypoxic water of 1.5–3.5 ml l⁻¹ becomes increasingly prevalent in the pelagic zones above the core ETA OMZ, this is likely to induce threshold physiological and behavioural responses of pelagic fishes leading to abundance and distributional changes (Lowe et al., 2000; Eka

et al., 2010), including those of sharks (Sims, 2019). In spite of this, no specialized studies have been carried out on the foraging pattern of these species in the OMZs and their susceptibility to fisheries.

Several studies have been carried out on the biogeochemistry of the OMZs, as well as a few simulations of top marine predators in hypoxia. Still, little is known about how top pelagic predators and large marine megafauna react when exposed to OMZs or hypoxia in their natural habit (oceans). OMZs are spread throughout the world oceans, but conditions differ even with the same latitudes of the world ocean and with very little study carried out in the North Atlantic.

This study attempts to analyse novel data on top marine predators' behaviour and habitat use in their natural habitat. It identifies the foraging and dive patterns of these top predators in relation to OMZs. It also reveals the relationship between fisheries and shark's foraging patterns in the OMZs with the potential to give policymakers more precise information on how ocean deoxygenation impacts the top marine predators and species.

1.3 Research Objectives

The main objective of this study is to provide the first quality information on the movements, behaviour and habitat preferences of blue and shortfin mako sharks in the North Atlantic with regard to oxygen concentration and fishing effort.

The specific objectives of the study will;

1. Compare the CMEMS model data with in situ data from the GLODAP to identify drifts in retrieved data from modelled environmental fields and characterize shark behaviour in relation to different oxygen gradients in the Central North Atlantic and the Eastern Tropical Atlantic Ocean OMZ.
2. Identify and characterize areas of putative foraging (shark aggregation) to determine the relationship between the foraging pattern of these pelagic sharks and habitat use in the central North Atlantic and the hypoxic areas of the ETA Ocean.
3. Investigate the extent of the hypoxia-based potential habitat compression to determine the correlation between blue and shortfin mako sharks' habitat use and their vulnerabilities to fisheries.

4. Examine the consequences and possible causes of OMZs relative to the ecology of these species and the fisheries that exploit them.

1.4 Research Hypothesis

The study hypothesizes that the foraging patterns and increased aggregation of pelagic sharks in the OMZs are due to the area's productivity. This could increase their susceptibility to capture by surface longline fisheries.

1.5 Relevance and Importance of the Research

One of the century's main concerns is climate change's impact on ocean warming, deoxygenation and fisheries, which may impact the ocean's top predators. However, a broad research gap exists in these ocean fish species' direct interaction and impact on the OMZ and their habitat.

This study will reveal the unknowns about the wild habitat use of two of the ocean's top predators in the OMZs and how this may have been a response to global warming or oxygen deoxygenation. This will enable policymakers to focus on the significance and steps to reduce human-induced climate change phenomena to protect these threatened ocean species.

A possible overlap of fisheries and shark occupancy in the OMZ in this study will inform conservationists about their risk and vulnerabilities to exploitation or overexploitation. The findings from this study will contribute to modelling studies which will establish and predict the effects of future warming and OMZ expansion on fish niches and determine how these may shift distributions and alter their vulnerability to fishing exploitation. Finally, this study will significantly reinforce the need for adequately implementing policies regarding marine protected areas for biodiversity conservation.

1.6 Structure of the Work

This research work consists of six sections. Section one includes the Introduction, which discusses the background to the study with a brief introduction to dissolved oxygen and OMZs in the world's oceans, and the vulnerabilities of the leading marine predators (pelagic sharks). This was followed by the problem statement, which revealed the underlying issues related to the topic. The main research goal, as well as the specific aims of the study, were outlined, followed by a research hypothesis revolving around the

study's main purpose. Finally, the meaning and importance of this study, as well as the structure of this work, were presented.

Section two begins with a definition of OMZs, and describes the variation in depth of OMZs. It also explains the expansion of OMZs while revealing the possible causes for the expansion of OMZs, consequences of oxygen minimum zone expansion, and habitat compression. This section summarizes what is already known about fish behaviour and physiological adaptations to low oxygen levels, foraging fish species in OMZs and the study preference of blue and shortfin mako sharks.

The third section of this study explains the methods and materials used for the study. This includes the need for the field of study. It also describes the types of data collected, the methods of data collection, and the methods used to analyze the data. The fourth section of this study consists of the results obtained based on each of the objectives of this study, while the fifth section of this study discusses the results obtained as well as criticisms and connections with previous studies. The final remark was presented in the sixth section of this thesis.

2. Literature Review

2.1 Oxygen Minimum Zones (OMZs)

An all-encompassing and straightforward definition of an OMZ based on absolute oxygen concentrations is unrealistic because no particular oxygen concentration defines a universal level of hypoxic stress for marine organisms (Seibel, 2011). OMZs in the eastern Atlantic, which is the primary focus of this review, are classified by an oxygen saturation level that is less than ~10% of that at the sea surface which corresponds to an oxygen concentration of $<20 \mu\text{mol kg}^{-1}$ (0.5 ml l^{-1} or 0.7 mg l^{-1}) (Levin, 2003; Helly & Levin, 2004; Paulmier & Ruiz-Pino, 2009). Such low oxygen levels are highly hypoxic for most known large organisms living in such strong OMZs, and they exhibit a variety of adaptations to hypoxia (Childress, 1995; Childress & Seibel, 1998; Drazen & Seibel, 2007; Seibel, 2011).

Whereas this definition of an OMZ based on microbial movement is non-arbitrary and valuable within the eastern Pacific and Indian Oceans (Fig 2.1A) (Lauvset et al., 2021), it is not universally applicable. Unmistakable OMZs exist within the eastern Atlantic, as shown in Fig 2.1B (Stramma et al., 2008), but the oxygen concentration in the core of the strongest Atlantic OMZ is $>20 \mu\text{mol kg}^{-1}$, which is considerably higher than those in the Pacific and Indian Ocean OMZs, where the oxygen level can be as low as zero (Karstensen et al., 2008; Canfield et al., 2010). This complicates recognizing a particular oxygen boundary for Atlantic OMZs, but a concentration of $<45 \mu\text{mol kg}^{-1}$ has been proposed to characterize OMZs (Karstensen et al., 2008). These definitions of an OMZ are consistent with physiological data indicating that an oxygen concentration range of $60\text{--}120 \mu\text{mol kg}^{-1}$ is seriously hypoxic for several marine organisms (Diaz & Rosenberg 1995; Miller et al., 2002; Vaquer-Sunyer & Duarte 2008). Therefore, the lower end of this range leads to hypoxic stress for several marine organisms (Seibel, 2011) and has often been used to define hypoxic habitats at depth (Whitney et al., 2007; Keeling et al., 2010).

In the Pacific and Indian Oceans, one can therefore use an oxygen concentration of $<60 \mu\text{mol kg}^{-1}$ to define the hypoxic regions above and below an OMZ's vertical boundaries as oxygen-limited zones (OLZs). This is the region immediately above or below an OMZ with an oxygen concentration of $<60 \mu\text{mol kg}^{-1}$ in the Pacific and Indian Oceans (Fig 2.1A) or $<90 \mu\text{mol kg}^{-1}$ in the Atlantic Ocean (Fig 2.1B) (Gilly et al., 2012;

Gilly et al., 2013). These regions are sometimes referred to as oxyclines, but this term is obviously vague. An oxygen concentration of $<90 \mu\text{mol kg}^{-1}$ has been proposed to define analogous OLZs in the eastern Atlantic Ocean (Karstensen et al., 2008).

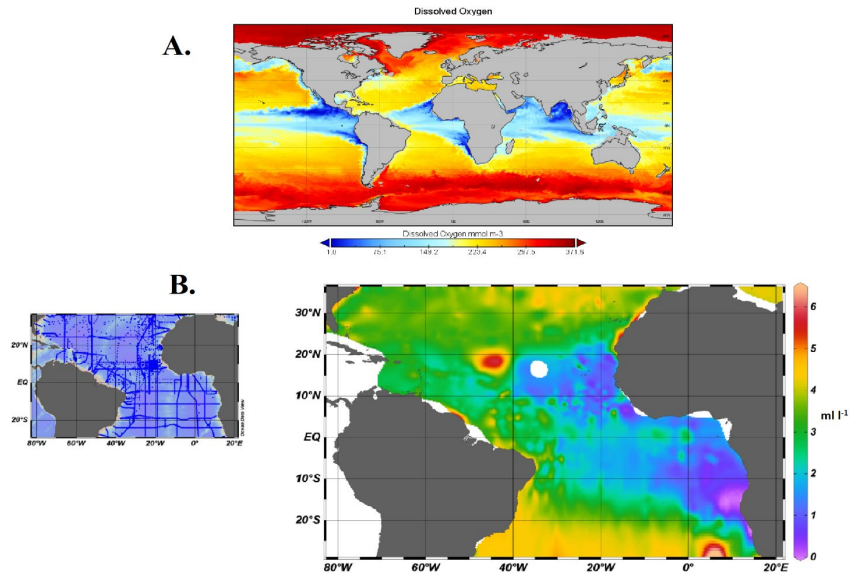


Figure 2. 1: Oceanic OMZs (A) CMEMS Global Modelled Integrated dissolved oxygen concentrations from 0 m to 200 m depth in the water column. (B) Visual interpolation of the mean in-situ acquired integrated oxygen concentration from 0 m to 200 m depth (GLODAP 2021)

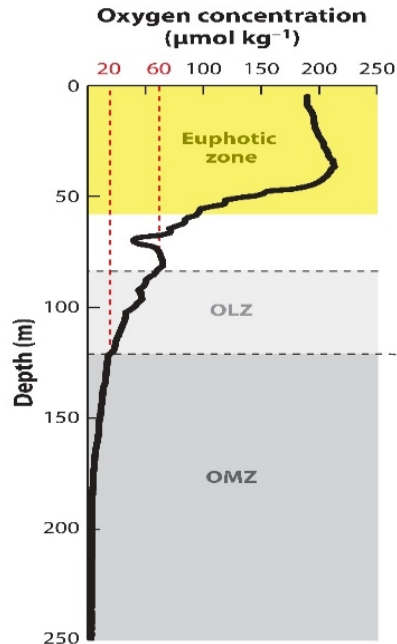


Figure 2. 2: Microbial biogeochemical processes active in OMZs and the oxygenated ocean. Characteristic depth profile for dissolved oxygen in the eastern tropical North Atlantic (Beman et al., 2012; Gilly et al., 2013), indicating the depths of the euphotic zone (yellow), oxygen limited zone (OLZ; light gray), and OMZ (dark gray).

2.1.1 Variation in Depth of Oxygen Minimum Zones

Since increasing pressure with depth affects the zoning of the continental margin (Carney, 2005) and temperature decreases with increasing depth up to 6000 m, the depth of the upper and lower limits of the OMZ and OLZ is a crucial feature. The flattest OMZs are found in the tropics, including the Gulf of California, the Pacific side of Mexico, and Peru; in the northern Indian Ocean; and on the Namibian shelf (Helly and Levin, 2004). In the Humboldt and Benguela currents, the OMZ begins at shelf and overhang depths (Arntz et al., 2006). These shallow OMZs can have their upper OMZ limit at 50-100 m depth, meaning that highly hypoxic waters are near the surface (sometimes within the euphotic zone) and impact fish communities in shallower waters. For example, off the southwest coast of India near the city of Cochin, strongly hypoxic OMZ conditions are found at 20 m depth from mid-August to October (Banse, 1968). In contrast, the upper limit of OMZs occurs deeper at higher latitudes. The upper limit of the California Current OMZ begins at slope depths (400-500 m) (Arntz et al., 2006) and is at greater depths off Oregon, Washington and Canada (600-700 m) than off California (Helly and Levin, 2004).

Highly hypoxic waters can be found seasonally at inner shelf depths (20-50 m) in some of these areas, such as off Oregon (Grantham et al., 2004). The depth of the lower limit of the OMZ in the California Current, Humboldt Current and Benguela Current regions varies significantly (Arntz et al., 2006), with the lower limit occurring at the upper slope depths (200-400 m) off Chile and Namibia. It also extends deeper into Central America, Peru (500 m) and North America (900-1100 m) (Arntz et al., 2006). The lower limit of the OMZ is also found deeper (> 1000 m) in the southern Gulf of California, the eastern tropical Pacific from 8° N to 22° N, and the northern Arabian Sea and Bay of Bengal (Helly and Levin, 2004). Most OMZ waters occur at depths less than 1500 m (Kamykowski and Zentara, 1990).

2.1.2 Expansion of Oxygen Minimum Zones

Global fish shoaling of the upper OMZ boundaries has been observed in all major eastern boundary current OMZs (Whitney et al., 2007, Bograd et al., 2008, Stramma et al., 2008b) as well as strong OMZs (i.e. oxygen concentrations <20 mol kg⁻¹) in the Gulf from Bengal and the Arabian Sea (Stramma et al., 2010). In many cases, the lower OMZ boundaries have also shifted to greater depths (Stramma et al., 2008b), but this feature has not been monitored as frequently. Fish shoaling an upper OMZ boundary (and

lowering the lower boundary) thus increases the OMZ volume in a given area. In some cases, the minimum oxygen concentrations in the OMZ cores have also fallen, intensifying the OMZ (Chan et al., 2008, Stramma et al., 2008b). Keeling et al. (2010) have provided detailed tabular representations of oxygen depletion and volume change in various OMZs. OMZ fish shoaling also results in horizontal expansion as the geographic area encompassed by the top of the OMZ at a given depth increases. In the NE Pacific, OMZ depth varies with latitude (Helly & Levin 2004), with the upper limit at 150 m or less in the tropical regions, in contrast to 500-600 m north of central California (Fig 2.4). The OLZ (above the OMZ) tops and thicknesses also vary widely, and in tropical regions, there may be an overlap with the euphotic zone (Fig 2.4A) (Fuenzalida et al., 2009).

On a global scale, the maximum oxygen depletion at a depth of 200 m (generally near the upper OLZ limit of 60 mol kg⁻¹) has been about 0.5 mol kg⁻¹ per year over the OMZs in the Atlantic and East Equatorial Pacific since the 1960s (Stramma et al., 2010). Similarly, a rate of decrease occurred in the Gulf of Alaska during this period, corresponding to a 100 m beating of the upper OLZ limit (Whitney et al., 2007). Rates three to four times higher (at 200 m) were observed over a shorter period (1984-2006) in a more localized area, with the OLZ ceiling obscuring at 70 m in the Southern Bay of California and Namibia (Bograd et al. 2008).

Climate models predict a general decrease in oceanic dissolved oxygen concentration and a resulting expansion of the OMZs under global warming situations, with the largest decreases occurring in extratropical regions (Stramma et al., 2008). In the tropics, the models predict either a zonal mean oxygen increase at depths of about 200 to 1000 m in the Atlantic and Pacific Oceans or moderate zonal mean oxygen decreases (Kwiatkowski et al., 2019). The predicted oxygen changes in the thermocline waters result largely from solubility changes in the upstream headwaters, changes in the deeper waters are mainly due to reduced internal advection and sustained oxygen consumption from remineralization of sinking organic particles (Kwiatkowski et al., 2019).

2.1.3 Causes of Oxygen Minimum Zones Expansion

Total ocean oxygen (within a depth range of 100-1,000 m) is decreasing globally but at rates of 10% of those mentioned above for certain OMZ/OLZ environments (Helm et al., 2011, Stramma et al., 2012). This deoxygenation is mechanistically linked to the expansion of the OMZ, as the global decline in ocean oxygen levels will alter the

headwaters aerating the OMZs within the water column. This reduces subsurface mixing and the transfer of atmospheric oxygen into the water column. Changes in oceanic circulation patterns can also reduce aeration from the water column. These declines and their causes have been thoroughly studied (Keeling et al., 2010). These conclusions are largely based on modelling approaches that predict that global oxygen depletion will continue in the future (Keeling et al., 2010).

Although physical impacts of climate change and multidecadal oscillations are believed to be the main drivers of ocean deoxygenation and OMZ expansion, biological mechanisms are also relevant. Oxygen depletion is therefore influenced by some processes that collectively determine the progression of depletion in different ocean regions and general link deoxygenation to OMZ expansion (Stramma et al., 2012). Primary production is key. Higher surface productivity produces more organic matter eventually consumed by midwater microbial communities, and increased surface production may stimulate oxygen depletion at depth. Primary production may increase in large parts of the world ocean (Chavez et al., 2011). Still, other studies have identified a global decline in phytoplankton biomass over the last century (Boyce et al., 2010). Regardless of the mean global trend, there are critical differences between specific ocean regions regarding changes in primary production.

Decreased production in oligotrophic regions of the open ocean could lead to a global decline in total production (Behrenfeld et al., 2006, Polovina et al., 2008, Doney et al., 2012), while production and phytoplankton biomass in overlying productive surface waters increase at the same time could OMZs (Gregg et al., 2005, Behrenfeld et al., 2006). These observations are consistent with the amplification of land-sea temperature gradients and coastal winds, resulting in increased coastal upwelling and production (Bakun et al., 2010, Doney et al., 2012). Physiological responses to warmer temperatures can result in increased surface production (Behrenfeld, 2011) and accelerated respiration of organic matter at depth since heterotrophic microbes can generally be more temperature-sensitive than phytoplankton (Wohlers et al., 2009, Sarmiento et al., 2010, Doney et al., 2012). Additional investigation of these biological drivers of deoxygenation and OMZ expansion is needed.

2.1.4 Oxygen Minimum Zones and Habitat Compression

Habitat loss associated with OMZs (hypoxia-based habitat compression) is characterized as the reduction of the oxygen-rich mixed layer at the shallow surface above a threshold of cold hypoxic water (Fig 2.5). As a benchmark, the OMZ is defined as the areas where the dissolved oxygen content below the thermocline is 3.5 ml l^{-1} (150 mol kg^{-1}) in relation to the species grouping (Brill, 1994; Roberts, 1978; Brill, 1996). This threshold has been reported (Brill, 1996; Prince and Goodyear, 2006; Price et al., 2010) as a plausible lower habitat limit for some tropical pelagic fish (Stramma et al., 2012) but brief deeper dives occasionally occur (Price et al., 2010). Although dissolved oxygen requirements vary in individual species depending on respiratory mode and metabolic and physiological requirements (Seibel, 2011), a dissolved oxygen level of 3.5 ml l^{-1} can induce stress symptoms in sharks and tuna with high oxygen requirements with prolonged exposure can be deadly. Possibly limiting their depth distribution to the oxygen-rich near-surface layer (Prince and Goodyear, 2006; Price et al., 2010).

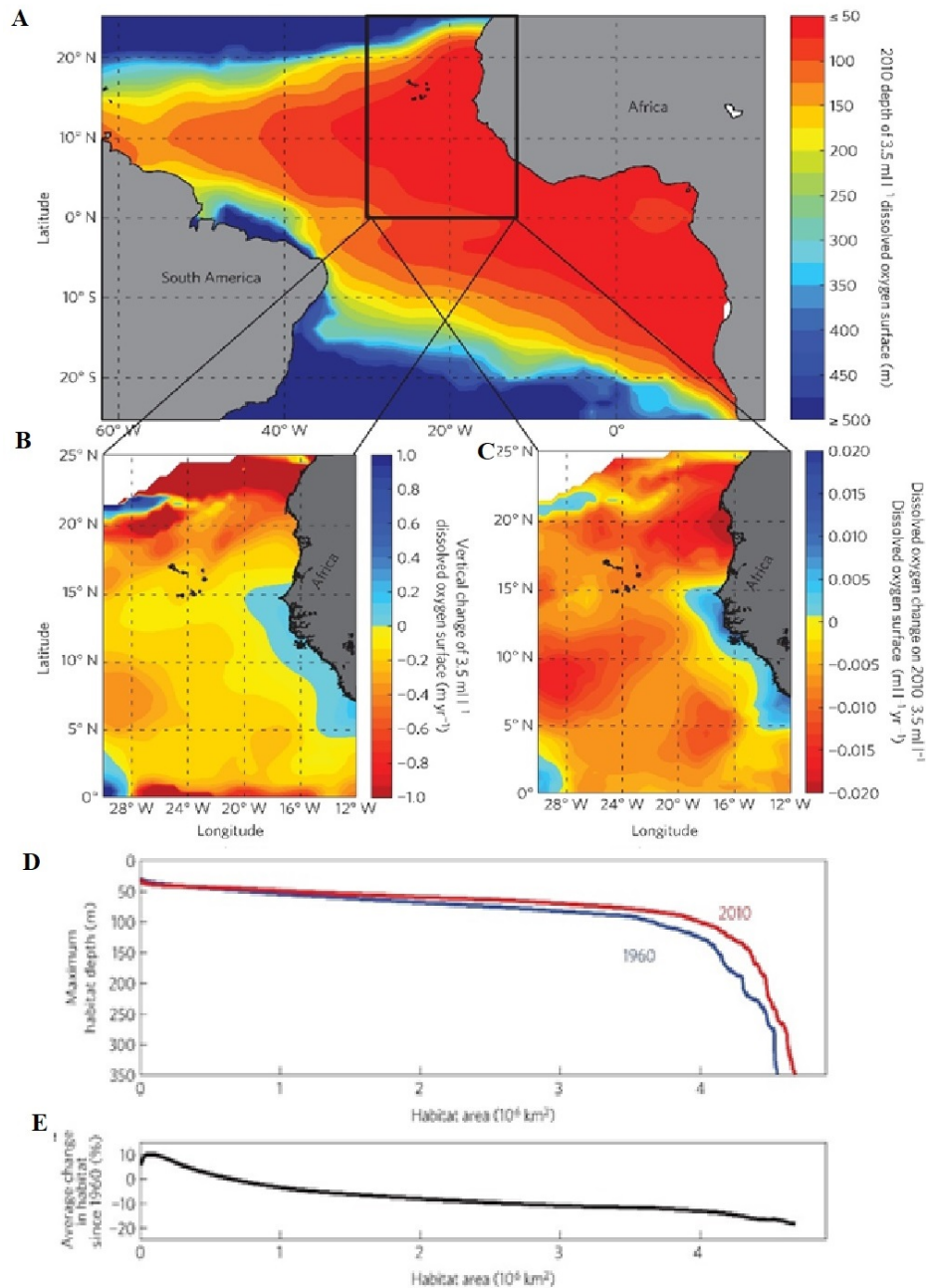


Figure 2. 3: Dissolved oxygen and habitat changes in the eastern Atlantic. (A) Depth of 3.5 ml l⁻¹ dissolved oxygen surface area (m) on January 1, 2010. (B) Average vertical change in 3.5 ml l⁻¹ dissolved oxygen surface area 1960-2009 (m yr⁻¹; blue indentation). (C) Change in dissolved oxygen (ml l⁻¹ year⁻¹) at depth of 3.5 ml l⁻¹ surface in 2010. D(E), summed area of sorted grid points by depth of 3.5 ml l⁻¹ dissolved oxygen content for the in B(D) and the corresponding average habitat loss relative to surface over the cumulative area due to the change in D(E). (Stramma et al., 2012)

2.1.5 Consequences of Oxygen Minimum Expansion

Although the oceanographic changes associated with OMZ expansion can be understood fairly well, we are less certain how individual species and ecosystems will be affected. Discussion of ecological responses has largely focused on benthic organisms inhabiting continental shelf environments and hypoxic basins (Levin 2003a, b; Levin et

al., 2009), with less attention given to pelagic organisms (Stramma et al., 2010). Hypoxia is closely related to thermal stress (Portner & Farrell 2008), and the interaction of these stressors applies to any environment affected by changing oxygen concentration or temperature. We assume that physical changes in the water column directly related to OMZ extension exert their effects primarily through oxygen concentration. Still, OMZ fish shoaling is accompanied by small temperature increases, particularly in the upper OLZ.

Temperature-related effects are more important at shallower depths. Since many midwater organisms transiently inhabit the near-surface epipelagic zone at night, decreasing oxygen and increasing temperature on mesopelagic organisms may prove more important than we currently suspect. The reduced oxygen can affect individual organisms in many ways, including acute physiological impairment, growth and reproductive success changes, and movement of mobile forms to more favourable oxygen regimes (either horizontal or vertical). At the ecosystem level, the different tolerances of different species to a changing environment will lead to differential interspecies success and concomitant changes in community structure and trophic networks. Effects of this latter type are inherently non-linear and extremely difficult to predict. We review here what is known about the effects of OMZ extension on selected non-benthic taxa, mainly in the eastern Pacific.

2.2 Behavioral and Physiological Adaptations of Fishes to Low Oxygen

There are many definitions of hypoxia (Hofmann et al., 2011), and the entire adaptation literature suggests multiple ways to become hypoxia-tolerant. This is consistent with the fact that hypoxia tolerance in fish has evolved independently many times (Friedman et al., 2012). Behavioural and morphological adaptations to hypoxia are briefly discussed here to better understand some of the patterns of changes in fish community abundance and diversity under OMZ conditions explored earlier in this section. Understanding which adaptations confer tolerance to hypoxia is important to understanding which fish species will be resilient to life in a more oxygen-deficient future ocean.

2.2.1 Responses of Oxygen Minimum Zone Species to Hypoxic Conditions

Two theoretical, but not mutually exclusive, mechanisms have been proposed in the literature as methods to cope with the reduced oxygen availability: increased oxygen removal from the environment (through increased gill surface area, ventilation behaviour,

increased oxygen affinity in airway pigments or other molecular changes), or reduced oxygen demand (through metabolic suppression or anaerobic metabolism) (Childress and Seibel, 1998; Friedman et al., 2012; Seibel, 2011).

Hypoxia-tolerant cellular systems respond to anoxia in two phases; defence and rescue (Hochachka et al., 1996). The first step involves suppressing ATP-demand and ATP-supply pathways by downregulating protein synthesis through translational arrest and downregulating ion channel ATP utilization through channel arrest (Hochachka et al., 1996). It is believed that cells that are not hypoxia-tolerant fail to recover from this translational protein synthesis arrest. In contrast, hypoxia-tolerant cells respond to prolonged periods of hypoxia by activating rescue mechanisms that begin to regulate the expression of several key proteins, enabling low-level metabolic activity but with dramatically reduced ATP turnover rates (Hochachka et al., 1996). Heme-based proteins, known to sense changes in oxygen tension in numerous organisms, are thought to be the oxygen sensors responsible for detecting hypoxic states and the subsequent activation of hypoxia-dependent transcription factors (Bunn and Poyton, 1996). In both fish and mammals, a heterodimeric transcription factor called hypoxia-inducible factor 1 (HIF-1) regulates target genes that are activated under hypoxic conditions (Semenza, 1998). Although no research has been conducted to identify this response in OMZ fish species, it is the basic cellular response to hypoxia likely to occur in these fish.

An increase in gill surface area under hypoxic conditions appears to be a common adaptation in different fish orders and is also a relatively plastic trait (Chapman et al., 2000), with changes in gill lamellar surface area occurring as rapidly as 12-24 h (Matey et al., 2008). *Nezumia liolepis*, a macrourid known to live under OMZ conditions in both the US West Coast OMZ and near Volcano 7 (Wishner et al., 1990, 1995), also had an enlarged gill surface (Friedman et al., 2012). A larger gill surface also appears to be an adaptation in cartilaginous fish, and the large head and expanded gills of the scyliorhinid, *C. cephalus*, are thought to be an adaptation to the severely hypoxic conditions. In contrast, other OMZ species in the order Scorpaeniformes show enzymatic adaptations to OMZ conditions. The sebastid, *S. alascanus*, has specific blood and cardiac enzyme adaptations that allow greater reliance on anaerobic metabolism (Gallo & Levin, 2016). However, it was found that enzymatic substrates for aerobic metabolism are reduced in both sebastids, *S. alascanus* and *S. altivelis*, indicating low aerobic activities under OMZ conditions (Friedman et al., 2012).

2.2.2 Behavioural Adaptations

Avoidance, altered respiration, decreased feeding, and altered phototaxis are all reported behaviours of fish in response to low oxygen levels (Davis, 1975). Changing breathing patterns, either through hyperventilation, increasing respiratory rate or stroke volume, or changing from periodic or episodic respiration to continuous respiration, are all possible responses of fish to hypoxia (Perry, 2011). Hyperventilation during hypoxia also produces respiratory alkalosis, leading to an increase in red blood cell pH, an increase in the hemoglobin affinity for oxygen through the Bohr effect, and an increase in O₂ uptake (Brauner and Randall, 1998). The Namib-dwelling gobiid OMZ, *S. bibarbatus*, can tolerate hypoxic conditions for long periods by increasing ventilation frequency.

OMZ tolerant fish may also exhibit habitat-specific behavioural adaptations, including microhabitat selection and semi-diurnal, diurnal, and seasonal migrations. For instance, OMZ species such as the sebastids, *S. alascanus*, and *S. altivelis* may prefer to utilize microhabitats exposed to greater water flow (e.g., the presence of rocks or hills that modify and enhance turbulence and currents). An orientation to the flow or the selection of microhabitats with stronger water flow over-breathing surfaces would increase gas exchange (Brewer and Hofmann, 2014).

There are also reports of fish exhibiting sluggish behaviour, reduced food intake and increased susceptibility to disease, and reduced immune responses in fish exposed to oxygen conditions slightly above lethal conditions (Shepard, 1955). It is unclear how OMZ conditions affect the immune responses of pelagic and demersal fish species living in OMZs. Fish living in OMZ conditions may be more susceptible to disease and parasites due to a reduced immune reaction. Grenadiers living in the Gulf of California OMZ appear to have a higher external parasite load than grenadiers observed in other areas.

2.3 Study Preference of Blue and Shortfin Mako sharks

Sharks are widely described by a complex spatial organization of their populations which has resulted from trade-offs between the components of their life history and social and environmental interactions (Klimley, 1987; Sims, 2005; Heupel et al., 2007). This complex organization is reflected in their sexual separation and the existence of discrete locations for key events during their life history, such as suckling and mating. In the context of declining shark populations (Ward, 2005; Dulvy et al., 2008) and their deleterious ecological effects (Ferretti et al., 2008), unravelling such spatial organization and, with it, accurately identifying essential fish habitats is key to developing appropriate

management plans for the protection of the most vulnerable life stages (Gruss et al., 2011). This need is most compelling considering our current limitations in understanding the impacts of heterogeneously distributed fishing pressure on spatially structured shark populations (Ward, 2005; Mucientes et al., 2008).

These two shark species are highly mobile predators able to migrate over thousands of kilometres in the North Atlantic Ocean (Kohler et al., 2002), with an average minimum dissolved oxygen requirement range between 1.7 ml L⁻¹ and 2.9 ml L⁻¹ (Nasby-Lucas et al., 2009). Shortfin mako (*Isurus oxyrinchus*) have been targeted in some areas for their valuable fins and meat and are also a relatively frequent catch of pelagic longline fisheries. These species are not as prolific as blue sharks, and there are concerns about their population status (Dulvy et al., 2008), with the shortfin mako shark species listed as endangered and the blue sharks as near threatened by the International Union for Conservation of Nature (IUCN) Red List.

2.3.1 The Blue Shark (*Prionace glauca*)

The blue shark (*Prionace glauca*, Carcharhinidae) is a marine water species worldwide in temperate and tropical waters. It is a unique shark with a slender, narrow body, long pectoral fins, indigo blue back colouration, metallic blue flanks, and sudden white undersides (Ferretti et al., 2008). It is the most abundant pelagic shark, and large numbers are caught by global fisheries, mainly as bycatch on longlines and in gillnets (Nakano & Stevens, 2009). The current status of blue shark populations is the subject of much debate (Mejuto, 1985). Blue sharks are very common locally and have a prolific life strategy with faster growth and a higher number of smaller offspring than other pelagic sharks (Simpfendorfer et al., 2002). This shark is an important part of the international shark fin trade (Clarke, 2003). Of all the pelagic sharks, it is the most carefully studied, with the most published information, of the Atlantic and North Pacific populations. Nakano and Seki (2003) summarised blue shark biological data concisely. Its wide geographical distribution, high initial abundance, and moderate productivity have earned the blue shark a reputation for being resilient to fishing pressure (Nakano & Stevens, 2009).

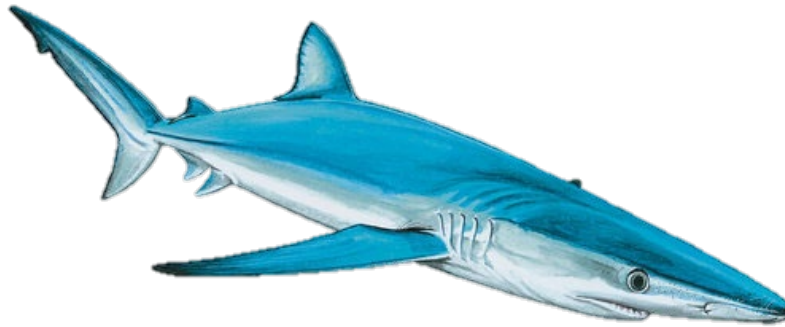


Figure 2. 4: Blue Shark (*Prionace glauca*) (Marylou, 2020a)

Biology and Ecological Status of Blue Shark

The age and growth have been relatively well studied in North Pacific, North and South Atlantic blue shark populations. Approximately half of the population of male blue sharks in the western Atlantic are sexually mature at a total length (TL) of 218 cm. However, some can reach maturity as short as 182cm. Females are subadult from 173 to 221cm TL and fully grown from 221 cm (Pratt, 1979). It was found that in the Gulf of Guinea and eastern Atlantic, half of the population of females were pregnant at 217 cm (Castro and Mejuto, 1995). In the North Pacific, maturity is about 200 cm TL for both sexes (Suda, 1953; Nakano et al., 1985). Pregnant sharks as small as 183cm have been recorded in the Northeast Pacific (Williams, 1977). In the South Pacific, males reach sexual maturity at about 229-235 cm and females at 205-229 cm (Francis and Duffy, 2005). Studies of blue shark ageing have generally used vortex rings, which appear relatively easy to read. Manning and Francis (2005) fitted some alternative growth models to data on length-age for blue sharks, preferring a snout model. It was found that females appear to approach a lower mean asymptotic maximum length and grow faster than males, in contrast to ageing studies using data from other oceans (Nakano & Stevens, 2009).

2.3.2 The Shortfin Mako shark (*Isurus oxyrinchus*)

Shortfin mako (*Isurus oxyrinchus*, Lamnidae) belongs to the most active and powerful of the fish and, like other members of the Lamnid family, is endothermic, consistent with the adaptations of scombrid tuna. This species is a popular sportfish and a common bycatch of pelagic longline fisheries, where it is retained for both meat and fin. Despite its frequent capture, the biology of the shortfin mako is not well known, with conflicting information on growth rates (Cailliet et al., 1983; Pratt and Casey, 1983) and relatively few captures of pregnant females resulting in gaps in our knowledge of the

reproductive cycle and the annual fertility (Mollet et al., 2000). As with other shark species commonly caught by longline fisheries, there are concerns about their population status, with recent literature suggesting significant declines in certain areas (Baum and Myers, 2004). The generally poor quality of data related to bycatch species creates problems in standardizing catch rates and makes it difficult to determine the impact of fishing on this species (and other pelagic sharks).

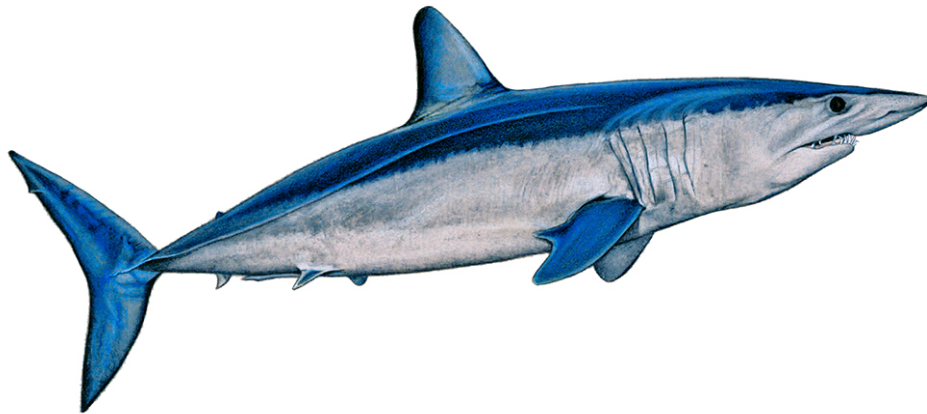


Figure 2. 5: Shortfin Mako shark (*Isurus oxyrinchus*) (Ines Fereira, 2020)

Biology and Ecological Status of Shortfin Mako shark

There is considerable uncertainty regarding the age and growth of the shortfin mako if one or two growth bands are produced every year (Cailliet et al., 1983; Pratt and Casey, 1983). Pratt and Casey (1983) assumed that two bands formed each year in the NE Atlantic, resulting in a relatively rapid growth rate, with maturity at around two and half years for the males (195 cm total length, TL) and six years for the females (265-280 cm TL). Cailliet et al. (1983) matured a small sample of shortfin mako from the Pacific and, assuming that a growth band was formed annually, reported a growth rate about half that of the Atlantic. The formation of one band per year now seems likely (Ardizzone et al., 2006), but stronger evidence awaits further investigation. The oldest fish was 17 years old, with an estimated lifespan of 45 years; The maximum size is about 4 m.

2.4 Past Studies

Ferretti et al. (2010) in his study emphasized the consequences of shark declines in the ocean as a result of the vulnerability of these apex predators to even light fishing pressure, and he opined that the decline of these large predatory sharks reduces natural

mortality in a range of prey, contributing to changes in abundance, distribution, and behaviour of small elasmobranchs, marine mammals, as well as sea turtles that have few other predators. In theory, the study also showed that large sharks could wield strong top-down forces with the potential to shape marine communities over large spatial and long temporal scales. This study agreed with Baum et al. (2003) on *the Collapse and conservation of shark populations in the Northwest Atlantic*, which showed a rapid decline in scalloped hammerhead, white, and thresher sharks by over 75% within the past 15 years.

Through the study carried out by Matzinger et al. (2007) on *thresholds of hypoxia for marine biodiversity*, they stressed that hypoxia is a mounting problem affecting the world's coastal waters, with dire costs for marine life which including death and catastrophic changes. A broad comparative analysis showed that although the hypoxia threshold varies greatly, the vast majority of studies and reports continue to use the 2-mg O₂/litre convention, initially derived as the oxygen threshold for fisheries collapse (Renaud, 1986). A number of published reports used the 2 mg O₂/litre and the 2 ml/litre (i.e., 2.85 mg O₂/litre) threshold, respectively, and a single study by Paerl (2006) used a threshold of 4 mg O₂/litre. A similar review by Gray et al. (2002) concluded that “mortality occurs where concentrations are below 2.0 to 0.5 mg O₂/litre”. The US Environmental Protection Agency (EPA) recommends a threshold of 2-3 mg O₂/litre for juvenile and adult aquatic organism survival (USEPA, 2000). A review carried out by Diaz and Rosenberg (2008) states that “hypoxia occurs when dissolved oxygen falls below 2 ml of O₂/litre resulting in high mortality when dissolved oxygen declines less than 0.5 ml of O₂/litre.” The results presented here show that the conventionally accepted level of two mg O₂/litre falls well below the oxygen thresholds for the more sensitive taxa. Nevertheless, all these are below the empirical sublethal and lethal O₂ limits for half of the species tested, which implies that the number and area of coastal ecosystems affected by hypoxia and, therefore, the future magnitude of hypoxia impacts on marine life have been largely underestimated.

A study of Ocean Deoxygenation in a Warming World carried out by Keeling et al. (2010) showed that ocean warming and increased stratification of the upper ocean caused by global climate change will likely cause declines in dissolved O₂ within the interior of the ocean (ocean deoxygenation) with consequences for ocean productivity, nutrient cycling, carbon cycling, and marine habitat as his model study predict a drop of

1 to 7% within the global ocean oxygen inventory over the subsequent century, with declines which will continue for a thousand years or more into the future with the consequence of an expansion within the area and volume of so-called OMZs.

Queiroz et al. (2016), in their study on Ocean-wide tracking of pelagic sharks, revealed the extent of overlap with longline fishing hotspots in the North Atlantic and validated that pelagic sharks occupy predictable habitat hotspots of high space use with 80% overlap of fished areas with hotspots, potentially increasing shark susceptibility to fishing exploitation in areas such as the North Atlantic Current/Labrador Current convergence zone and the Mid-Atlantic Ridge (MAR) southwest of the Azores.

In a study on the *Movements of electronically tagged Shortfin mako sharks (Isurus oxyrinchus) in the eastern North Pacific Ocean* carried out by Nasby-Lucas et al. (2019), a total of 105 Mako sharks tagged in the California Current between 2002 and 2014 revealed the immense distance covered by shortfin mako sharks (travelled in 1 year ranged from 6945 to 18,800 km/year) and also showing the strong correlation between seasonal movements of this species within the California Current based on primary productivity and chlorophyll a, and sea surface temperatures (SSTs) as an indicator of their foraging pattern. Miller et al. (2015) explored the quantifying associations of basking sharks and oceanographic fronts in the north-east Atlantic, which indicated that sharks show a preference for productive regions, and associate with contemporaneous thermal and chl-a fronts more frequently than could be expected at random, thereby correlating with their habitat occupation. It was also revealed that surface frontal activity is a predictor of basking shark presence in the northeast Atlantic, both over seasonal timescales and in near real-time, which gave a clear implication for understanding the preferred habitats of basking sharks in the context of anthropogenic threat management and marine spatial planning in the region.

A similar study by Queiroz et al. (2017) in the North Atlantic suggested that macropredator responded behaviourally in similar ways to environmental heterogeneity as fine-scale dive profiles of the shark species with varying feeding tactics may be utilized to identify key marine habitats. This includes foraging areas where sharks aggregate and which may represent target areas for conservation.

Bond et al. (2015), in an investigation on the *vertical and horizontal movements of a silvertip shark*, identified diel depth, temperature, and vertical habitat use differences

and concluded that diel depth differences and expanded daytime depth use could indicate foraging behaviour, routine predator avoidance, or temperature selection. Similarly, Abascal et al. (2011) carried out a novel study on the movements and environmental preferences of the shortfin mako, *Isurus oxyrinchus*, in the southeastern Pacific Ocean; they found out that the fish spent the most of their time in the mixed layer but undertook dives down to 888 m with no clear diel pattern in-depth behaviour was observed, but mean vertical distribution was deeper during the daytime which shows some contrast in the dive pattern of the two top marine predators (shortfin and silvertip shark).

In a similar vein, Coffey et al. (2017) undertook a study on the *oceanographic parameters which influenced the vertical distribution of a highly migratory endothermic shark (Lamna ditropis)* and identified key environmental factors that influence the vertical distribution of salmon shark; he observed that Diel shifts in vertical distribution, as well as behaviour, were consistently observed across their range and likely reflected shifts in their foraging ecology which corroborate Bond et al., (2015) and Abascal et al., (2011) studies. The sharks were also found to use a wide thermal niche and exhibited submergence behaviour, which could be linked to the thermal refuge when encountering sea surface temperatures outside their preferred temperature distribution, and they are also able to exploit low dissolved oxygen environments ($<1-3 \text{ ml l}^{-1}$), occasionally for extended periods of time in offshore habitats.

Howey et al. (2017) studied the *Biogeophysical and physiological processes that drive movement patterns* on 23 blue sharks with PSATs in the northwest Atlantic revealed that vertical behaviours displayed by blue sharks varied greatly among locales, and individuals exhibited a greater frequency of deep-diving behaviour. Also, the results reflect and support existing Atlantic migration models and highlight the complex, synergistic nature of factors which affects blue shark ecology and the need for a cooperative management approach in the North Atlantic, which corroborates the study carried out by Nasby-Lucas et al. (2019) on shortfin makos.

Various abiotic and biotic factors, which include temperature, CO₂, acidification, toxic metals and feeding that interact with hypoxia, are analyzed for their effect on P_{crit} (critical oxygen level). Rogers et al. (2016) investigated the hypoxia tolerance of fishes and how this varies among individuals and species. Their modelling opined that the ultimate partial pressure of CO₂ reached can vary from 650 to 3500 μatm depending on

the ambient pH and salinity, potentially affecting blood acid-base balance and P_{crit} itself. This observation was corroborated by Mandic et al. (2009). Likewise, Vedor et al. (2021) discovered through satellite-tracked blue sharks and environmental modelling in the ETA OMZ that shark maximum dive depths (MDD) decreased due to joint effects of declining DO at depth, high sea surface temperatures, and increased surface-layer net primary production which exposes these sharks to fisheries.

Prince et al. (2010) showed a contrast of dissolved oxygen (DO) and temperature profile in a study on the hypoxia-based habitat compression of tropical pelagic fishes between marlin and sailfish monitored with electronic tags where a cold hypoxic environment constitutes represents a lower habitat boundary limit in the ETP, ETP but not in the Western North Atlantic (WNA), (WNA) where DO is not limiting and non-constraining. He also suggested that sailfish in the eastern Pacific and eastern Atlantic sailfish are larger than those within the WNA, where the hypoxic zone is much deeper or absent. At the same time, he believed that larger sizes might reflect improved foraging opportunities offered by the closer proximity of predator and prey in a compressed habitat and higher productivity.

Penn et al. (2018) simulated greenhouse gas-induced global warming using a model of Earth's climate and coupled biogeochemical cycles consistent with geochemical proxy data and concluded that increases in atmospheric greenhouse gas levels reduced near-sea surface temperatures by more than $\sim 10^{\circ}\text{C}$ increases and decreases global marine O_2 levels by nearly 80%. A 50-year time-series study of the expanding OMZs in tropical oceans conducted by Stramma et al. (2008) revealed that over the past 50 years, oxygen in the 300 to 700-m layer has declined by 0.09 to 0.34 $\text{mmol kg}^{-1} \text{yr}^{-1}$, with negative consequences for ecosystems and coastal economies. Also, Stramma et al. (2012) confirmed habitat compression and associated potential habitat loss by electronic tagging data as the phenomenon increased the vulnerability of surface gear to top marine predators and opined that this is associated with a Global decline in pelagic species by 10-50% could be linked to predator diversity.

3. Materials and Methods

3.1 Study Area

This study covers the CAN and ETA with the northern boundary of 30° N, the southern boundary of 0° and the Western Boundary of 40° W and 0° (FAO area 34) with a depth range of 0 m to 2000 m. It was selected due to the presence of an OMZ in the region (Fig 2.1b, Fig 3.1). While OMZs expansion is not limited to the ETA, as discussed in section 2.2.5, the observed expansion trend is more pronounced in this area compared to other parts of the Atlantic Ocean. Consequently, oxygen concentrations from GLODAP and CMEMS in the North and South Atlantic were considered, while shark tracks were limited to the ETA within the boundaries mentioned above.

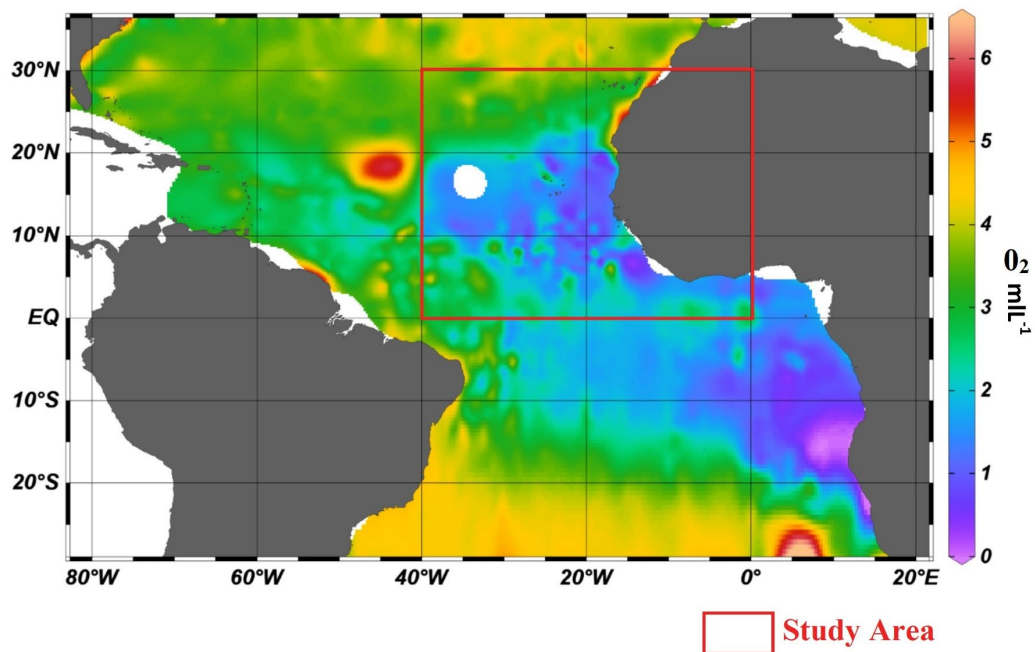


Figure 3. 1: Map showing the spatial extent of the study area overlaid on oxygen concentration at 100 m depth

3.2 Data Collection

3.2.1 Shark Data Collection

Data from PSATs attached on blue sharks (7 tags) and shortfin mako sharks (10 tags) tagged in the Central North Atlantic and ETA in 2011, 2017 and 2018 was used in this study with metadata displayed in Table 3.1 and mapped in Fig 3.2 and Fig 3.5.

Table 3. 1: Summary of satellite tag deployments on blue and shortfin mako sharks in the North Atlantic, including ID, track dates, and deployment locations decoded via satellite.

Shark	PTT	Sex	Pop-up time	Deployment Location		Track Duration	
				Lat (° N)	Long (° W)	Start	End
Blue (bl)	85140	M	120	42.375	29.45	22/08/2011	20/12/2011
	91026	F	90	42.35	28.1	21/08/2011	19/11/2011
	107085	F	120	32.375	36.125	28/08/2011	30/11/2011
	164441	F	90	13.5	28.475	24/01/2017	24/04/2017
	164442	F	120	14.2	28.425	26/01/2017	26/04/2017
	164443	M	90	13.85	28.4	25/01/2017	26/05/2017
	164444	M	120	15.1	28.4125	28/01/2017	29/05/2017
Mako (mk)	54552	-	-	22.625	24.65	7/12/2010	19/12/2011
	79794	-	-	23.125	20.75	11/12/2010	22/12/2010
	79802	-	-	22.4125	24.6	7/12/2010	3/1/2011
	79813	-	90	22.25	21.6	29/12/2010	20/06/2011
	107089	M	120	42.3	28.4	21/08/2011	19/12/2011
	164446	M	60	13.625	29.025	24/01/2017	21/03/2017
	164447	M	90	7.9	19.6	23/04/2018	25/06/2018
	164448	M	120	7.975	19.375	23/04/2018	6/6/2018
	164449	M	120	6.175	19.1	24/04/2018	23/06/2018
	164450	M	120	6.575	19.075	24/04/2018	18/05/2018

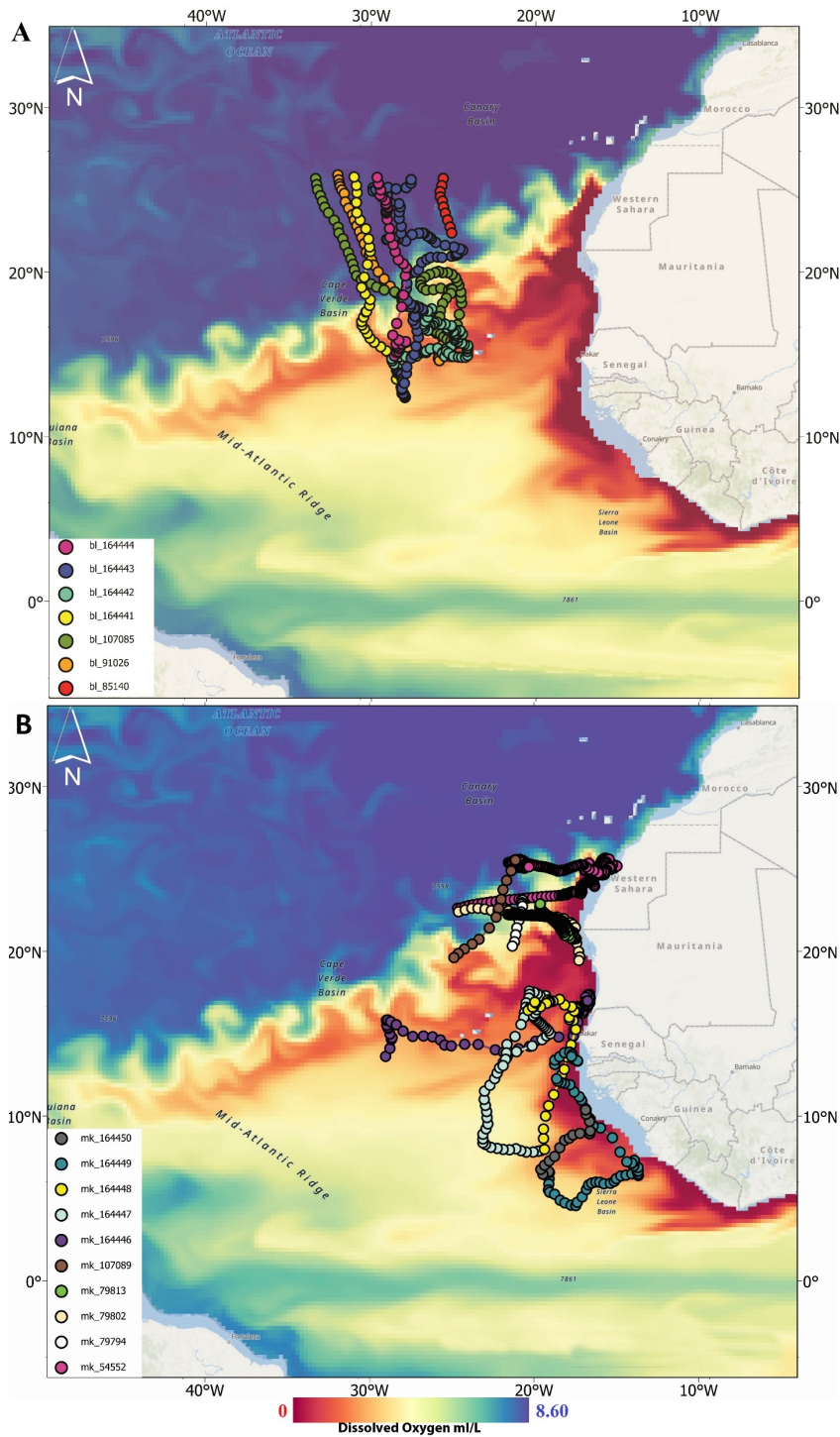


Figure 3. 2: North Atlantic-wide movements of (A) Blue and (B) Mako sharks in relation to the ETA dissolved oxygen at 100 m depth. Sharks were tracked PSATs (deployed in the western and central North Atlantic and above the ETA OMZ) superimposed on modelled dissolved oxygen concentrations (at 100 m).

Tag Description

The PSAT is a microcomputer that collects data on the water masses crossed by tagged animals (Fig 3.3). During the survey, PSATs were used as they logged temperature, depth (pressure), and light intensity after the shark was released, which can

then be used to calculate the latitude and longitude of the shark's position. The tags represent a fusiform cylinder of 124 mm (length) and 38 mm (diameter) with an antenna and anchor suit (Fig 3.3). The tags detach after a programmed interval and transmit their recorded information through the ARGOS satellite system to a land station, then ultimately to the researcher via the Internet. The full-functioning electronic tag is programmed to collect data on habitat and migratory behaviour.

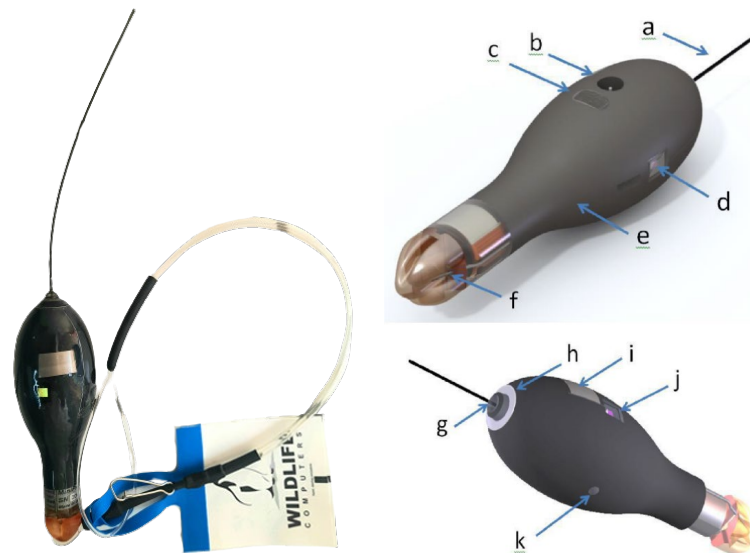


Figure 3. 3: MiniPAT tag showing: (A) Argos antenna, (B) temperature sensor, (C) communications port with plug, (D) light sensor (1 of 2), (E) float, (F) release pin, (G) LED light, (H) wet/dry sensor, (I) ground plate, (J) light sensor (2 of 2), (K) pressure sensor (Source: Wildlife Computers, 2016, 2017).

MiniPAT tags have three states which are start, auto start, and the stop phases. When in start mode, a tag is running and begins its deployment while auto start allows the tag to start by submersion in seawater and in the stop state, the tag will remain unresponsive unless connected to a computer via the tag management software ‘Tag Agent’. Stop mode is used to store tags for periods longer than a month (Wildlife Computers, 2016). However, onboard the vessel, tags were stored in auto start mode irrespective of cruise duration but when in auto start state, the tag will switch to start state as soon as it is submerged in salt water.

Shark Tagging Process

The sharks were caught on commercial baited longlines and brought alongside the vessel at the gear transport stage, lifted and tagged.) PSATs were manipulated with a

monofilament tether covered with silicone tubing and looped through a small hole in the base of the first dorsal fin. as shown in Fig. 3.4 below.

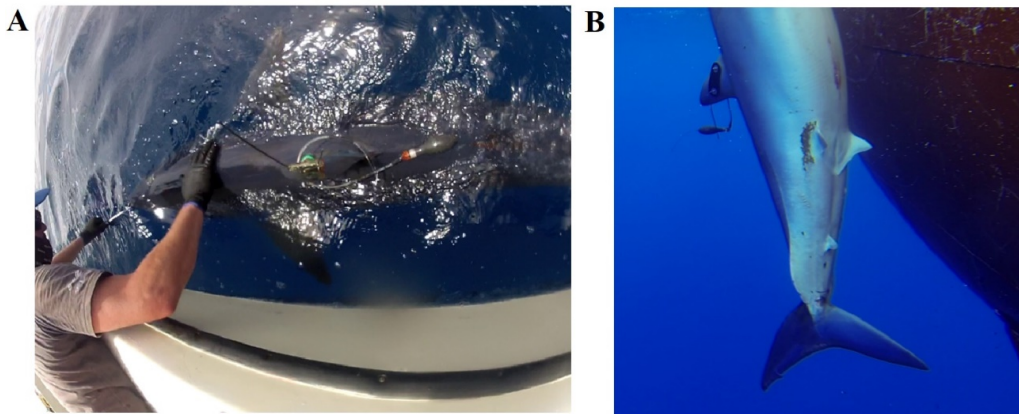


Figure 3. 4: Process of shark tagging PSAT rigged through the dorsal fin of a Mako shark from two different sides of the boat

Geolocation of the sharks tagged

Transmitted PSAT data were decoded with manufacturer software, and light-based geolocations were estimated using GPE3 software (Wildlife Computers, Inc.) and quality checked before analysis. The GPE3 model is based partly on previous work by Pedersen et al. (2008) that used hidden Markov models to geolocate Atlantic cod. The approach uses the archived tag data (light level, depth, and temperature) and corresponding sea surface temperature (NOAA OI SST V2 High Resolution) and bathymetry reference data (ETOPO1-Bedrock) in a gridded hidden Markov model (HMM, WC-GPE3, Wildlife Computers) to generate a most probable track (MPT) and associated uncertainty. Light level data were examined to ensure that each track recorded only single-time estimates of dawn and dusk per day. Where duplicate estimates were presented for either event, the later time was removed from the dataset.

3.2.2 Environmental Data

Copernicus Marine Environment Monitoring Service Data (CMEMS)

This study's two model data products were the Global Ocean Biogeochemistry hindcast (GLOBAL_MULTIYEAR_BGC_001_029) and the Global Ocean Ensemble Physics Reanalysis (GLOBAL_MULTIYEAR_PHY_001_031). The Global Ocean Ensemble Physics Reanalysis is a 3D potential temperature, salinity and currents reanalysis from top to bottom, which contains physical state variables of the ocean like

seawater temperature ($^{\circ}\text{C}$), seawater salinity (PSU), sea surface level/height (m), seawater velocity (ms^{-1}), mixed-layer thickness (m). The daily mean of Sea Surface Temperature (SST) was used in this study with a spatial resolution of $0.25^{\circ} \times 0.25^{\circ}$ regular grid. The CMEMS Global Ocean Ensemble Reanalysis product was improved with data assimilation using data from satellite and in-situ observations. It contains four reanalyses, namely GLORYS2V4 by Mercator Ocean (France), ORAS5 by European Centre for Medium-Range Weather Forecast (ECMWF), GloSea5 by Met Office (UK) and C-GLORSv7 by Centro Euro-Mediterraneo Sui Cambiamenti Climatici (CMCC) (Italy) of which the GLORYS2V4 was selected for this study. It spans a period from 01-01-1993 to 31-12-2019. Temperature data from 2011, 2017 and 2018 were selected for this study.

The Global Ocean biogeochemistry hindcast is a multiyear 3D hindcast biogeochemical product with no data assimilation. Like the Global Ocean Ensemble Reanalysis product, this globally available biogeochemical product is produced by Mercator-Ocean (Lamouroux et al., 2019; Perruche et al., 2019). The daily product used in this study contains six variables vis-à-vis dissolved oxygen (DO) in mmol. m^{-3} , chlorophyll (Chl) in mg m^{-3} , net primary production (NPPV) in mg.m^{-3} , silicate (Sil) in mmol. m^{-3} , nitrate (NO_3) in mmol. m^{-3} and phosphate (PO_4) in mmol. m^{-3} in which will DO mmol. m^{-3} , chlorophyll-a concentration ($\mu\text{mol l}^{-1}$), phytoplankton concentration ($\mu\text{mol l}^{-1}$), and net primary productivity ($\text{g l}^{-1} \text{d}^{-1}$) were used in this study with a temporal coverage of from 1993-01-01 to 2020-12-31 and a spatial resolution of $0.25^{\circ} \times 0.25^{\circ}$ regular grid. Dissolved oxygen and chlorophyll-a environmental variables correlated with the shark track dates in 2011, 2017 and 2018 were extracted from the surface to 2000 m depth. To account for the spatial error around shark individual geolocations, the data were therefore averaged for 1.25° in latitude as well as 0.75° in longitude (using a 5×3 grid cell) around each position (Vedor et al., 2021).

Units of Environmental Fields

Oxygen

Molar volume at STP = 22.391 l

Molar weight of oxygen = 31.998 g

Atomic Mass of oxygen = 15.994 g/mol

1 $\mu\text{mol O}_2$ = 0.022391 ml

1 ml/L = $1000/22.391 = 44.661 \mu\text{mol/L}$

1 ml/L = 1mmol/m³ divided by 44.661 $\mu\text{mol/l}$

$$1 \text{ mg/L} = 22.391 \text{ ml}/31.998 = 0.700 \text{ ml/L}$$

$$1 \text{ mg-at/l} = 15.994 \times 22.391 / 31.998 = 11.192 \text{ ml}$$

The spatial geolocation error of shark tracking was accounted for by averaging the pO₂ for 1.25° latitude and 0.75° longitude around each shark location.

Temperature

The temperature unit used for this study was °C

Chlorophyll-a

The Chlorophyll-a concentration unit used for this study was μmol l⁻¹.

Global Ocean Data Analysis Project (GLODAP)

The GLODAP (GLODAPv2.2021) data used were biogeochemical bottle data from the surface to the bottom of the ocean, with a focus on seawater inorganic carbon chemistry and related variables determined by chemical analysis of seawater samples (Lauvset et al., 2021). GLODAP started in 2004 as a result of the collaboration between scientists from the WOCE, JGOFS, and OACES, who can synthesize in situ biogeochemical bottle data into easily usable and readily available products (Key et al., 2004), thereby providing the first global accurate and precise seawater sample data worldwide. The GLODAP data used for this study included measurements from more than 400,000 water samples from the Atlantic Ocean collected on more than 300 cruises span 48 years from 1972 to 2020 between a depth of 0 m to 6000 m. Data for the twelve core variables (salinity, oxygen, nitrate, silicate, phosphate, dissolved inorganic carbon, total alkalinity, pH, CFC 11, CFC 12, CFC 113, and CCl₄) have undergone extensive quality control, especially systematic evaluation of bias (Olsen et al., 2020; Lauvset et al., 2021).

The data are available in two formats: one as it was submitted by the data originator but updated to WOCE exchange format and two, as a merged data product with adjustments applied to minimize bias, but the latter was used for this study with emphasis on oxygen concentration and depth in order to achieve the first objective and as a support data to achieve other objectives. The units used followed the same conversion factors as in the CMEMS.

3.2.3 Fishing Effort Geolocation

The latest version (2.0) of the Global Fishing Watch Automatic Identification System (AIS) based on fishing effort and vessel presence datasets which spans 8 years between 2012 and 2020, was used for this study along with the PSATs data to correlate

the spatial overlap of the shark with fishing effort. The fishing effort data were binned into grid cells of 0.01degrees and measured in units of hours (hours of fishing). The Automatic Identification System was developed as a vessel safety and anti-collision system with global coverage and not explicitly to track fishing vessels for fishery management purposes. However, its global coverage of the locations of many thousands of ships through time enables the analysis of the distribution of fishing efforts (Kroodsma et al., 2018a; Kroodsma et al., 2018b; Shepperson et al., 2018). GFW uses two neural network algorithms to categorize different types of fishing gear (for example, drifting longlines or purse seines). In addition, it estimates the spatiotemporal locations at which fishing gears were most likely to be deployed by individual vessels (Kroodsma et al., 2018a; Kroodsma et al., 2018b; Shepperson et al., 2018; Queiroz et al., 2019). GFW gridded fishing-effort data between 2012 to 2020 for drifting pelagic longlines was used for this study.

3.3 Method of Data Analysis

3.3.1 GLODAP and CMEMS Data Integration

Daily modelled oxygen data with a spatial grid of 1° x 1° were taken from the CMEMS Global Ocean Biogeochemistry hindcast (Global_Multiyear_BGC_001_029) for the North and South Atlantic Ocean for the years 2011, 2017 and 2018, while the same was selected for the GLODAP. Through the use of R programming language as a tool for the data extraction and analysis, the modelled data were extracted at all depths (0 m to 2000 m) and dates, matching the real individual locations of the GLODAP, while the unique in-situ data acquisition stations were also taken into account as the structure of the GLODAP indicated samplings carried out in different stations on the same day. Oxygen values interpolation was done for the target depth of GLODAP where oxygen concentrations were not available for CMEMS data in order to obtain spatial and temporal corresponding data for further analysis.

3.3.2 Statistical Analysis

Oxygen concentration fields from both Models were subjected to a statistical test to obtain the drift and correlation between oxygen concentrations at the same depth and dates in the north and south Atlantic. A pairwise two-sample t-test was performed using the `t_test()` function in the `rstatix` package in R, at a significance level of 0.05 to test if

there exists a significant or non-significant spatial/temporal/depth difference between the oxygen concentrations of both in-situ and modelled data. Furthermore, the Root mean square error between the two models was carried out to evaluate the reliability and accuracies of the two models as defined below.

$$\text{RMSE} = \frac{\sqrt{\frac{1}{N} \sum_{i=1}^N (E_i - O_i)^2}}{N} \quad (\text{Eq.1})$$

Where E_i is the i th GLODAP data, O_i is the i th CMEMS data and N is the number of observations available for the analysis.

The RMSE parameter can be decomposed in its components proportional to the average deviation between the CMEMS and GLODAP series and the scatter of the values around the average (Mentaschi et al., 2013a; Mentaschi et al., 2013b; Pasqualotto et al., 2019). This decomposition provides a geometrical insight into whether a bias exists, which can be attributed to a dependency between the two components.

The Scatter index (SI) is defined as the Root mean square deviation between the CMEMS and the GLODAP series subtracted from their average values in the equation below.

$$\text{SI} = \frac{\sqrt{\sum_{i=1}^N [(E_i - \bar{E}) - (O_i - \bar{O})]^2}}{\sum_{i=1}^N O_i^2} \quad (\text{Eq.2})$$

where \bar{E} and \bar{O} are the average GLODAP and CMEMS values respectively.

The Scatter index (SI) is a normalized measure of error, often reported as a percent. Lower values of the SI are an indication of better model performance. In the case of unbiased model runs, SI and RMSE coincide. It can be easily shown that the RMSE can be expressed as the quadratic sum of the scatter component and the bias BI (which is an index of the average component of the error. A value closer to zero identifies a better simulation), which validates both models and in turn be used to associate the behaviour of the sharks.

A correlation coefficient run was performed on both models as defined below.

$$\sigma = \frac{1}{N} \frac{\sqrt{\sum_{i=1}^N (E_i - \bar{E})(O_i - \bar{O})}}{\sigma_E \sigma_O} \quad (\text{Eq.3})$$

where σE and σO are the standard deviations of the GLODAP and the CMEMS, respectively. This quantity, which ranges between -1 and 1 , is an index of the scatter component of the error, and a value closer to 1 indicates a smaller scatter of the CMEMS values around the GLODAP.

This statistical analysis was applied to two model data across the Atlantic after data integration and study area between 40° W, 0 , 30° N, and 0 , where the OMZs were observed.

3.3.3 Environmental Integration of Oxygen with Shark Movement Data

Exploratory data technique on the two models' data with the shark movement data was carried out to access the response of individual sharks on different days to oxygen concentrations. A latitudinal extent of 30° N, 0° and longitudinal extent of 40° W and 0 were defined as the study area (Fig 3.4) due to the matching criteria we set, which correlates shark locations (with unique days) with the environmental fields (oxygen concentration) between a depth of 0 to 2000 m.

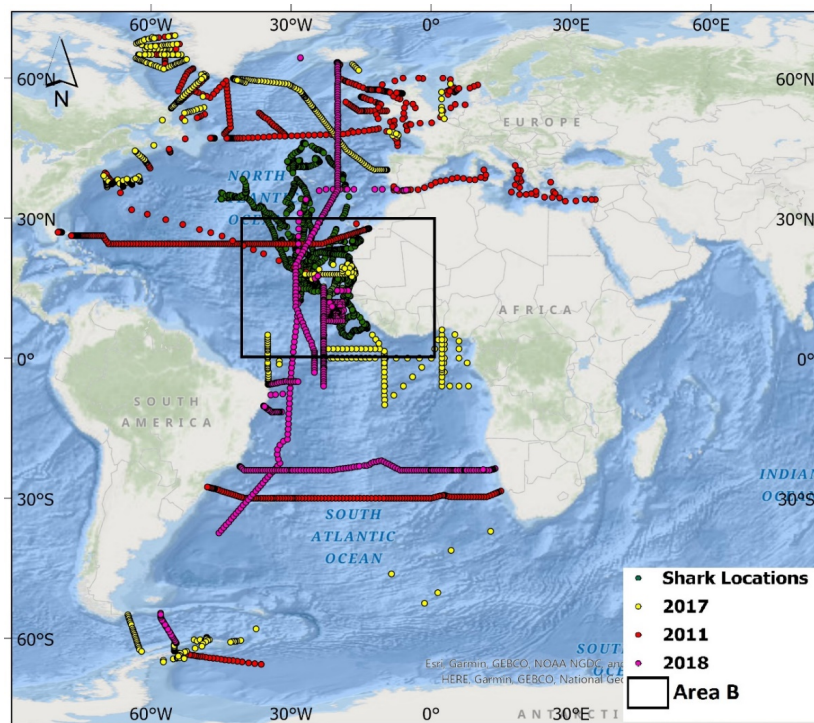


Figure 3. 5: Map distribution of the complete tracks of sharks, study area and GLODAP data geolocation across the Atlantic Ocean

Three datasets of oxygen concentrations were obtained using a matching algorithm which extracts CMEMS oxygen concentration on the shark position and

GLODAP position within a 2.5° radius of the shark positions on any given day. These oxygen concentrations were retrieved through three different methods from the two models (*Cmems_shark*, *Glodap_Shark* and *Glodap_Cmems_Shark*) were coupled with the MDD of the shark at a given date to determine their dive patterns with respect to oxygen concentrations along their tracks. Outliers above 95% quantile, i.e. 2.5°, were removed for the latter to avoid non-uniformity in oxygen values and gradient around the closest shark position (See appendix 1).

3.3.4 Mapping Shark distribution and the Environment

For the spatial analysis of shark horizontal movements in Area B (Fig 3.5), individual shark tracks (geolocations) and environmental data such as daily mean chlorophyll, temperature and oxygen concentrations at a depth of 0 m and 100 m, respectively, were integrated using ArcGis Pro.

Kernel density estimators have been used successfully in many tracking studies to describe habitat use and to identify areas of high marine animal use (Block. Et, al., 2005; Wood et al., 2000). However, when using this technique to quantify utilization distributions from tracking data, care needs to be taken to consider biases and ensure transparency and objectivity (Walli et al., 2009; Queiroz et al., 2016). Therefore, to identify areas with a high probability of foraging, interpolated data points were also used to calculate shark space use by performing a kernel density estimate in ArcGIS (spatial analyst/kernel density).

Using 1° x 1° grid cell as unit area, distribution probabilities were calculated from the estimated geolocations using a tracking effort-weighted kernel density analysis to derive an index of shark residence probability per unit area, to identify areas of multi-individual high utilization and to obtain real occupancy within these areas through the extraction of the tracking data. The number of shark residents in an area at a time was determined and the number of days spent in an area. Additionally, the mean number of days which shows the residence or occupancy days of groups, was obtained.

Due to the single deployment location of blue sharks in this study and the varying individual tracking durations, the number of tracked animals decreases randomly with distance from the deployment location, depicting a sampling bias towards the Northwest Atlantic. In this region, the grid for the geolocation estimates showed very high densities around the tagging location in Sao Vicente, Cabo Verde. This was accounted for by normalizing the skewed density estimate of days tracked in each cell by dividing it by the

number of individual Blue/Mako sharks tracked within each cell (Fig 4.6). The resulting index reflects a mean probability of shark residency (mean days) over the area with respect to environmental fields (Fig 4.7; 4.8; 4.9).

3.3.5 Shark and Fishing Vessel Spatial overlap and effort

For each gear type in this study, the number of hours fishing in a month (expressed as days, in which 24 h of fishing effort = 1 day) within each $1^\circ \times 1^\circ$ grid cell were summed to provide 12 monthly global fishing-effort maps. The mean annual fishing effort per grid cell in a relative year was calculated from the 12 monthly fishing-effort maps (Queiroz et al., 2019).

The spatial overlap between shark distribution and fishing effort was calculated as the number of grid cells that sharks and fishing effort (in days) occurred in the same $1^\circ \times 1^\circ$ grid cells in an average month, as a function of all shark grid cells occupied and standardized for shark track length. This was summarized as the spatial overlap of shark residence time over the sum of the monthly fishing effort of the vessels. The residency in mean days of individual sharks that overlaps the fishing effort grid cells indicates a higher probability of shark exposure to fishing at a given period of time. The mean days and spatial overlap of an individual shark were determined by averaging the total number of days in a grid cell by the total number of sharks present in a grid cell at a given time for each species. This, in turn, was overlaid on the fishing effort grid cells and across all individuals of a species within each ocean region.

A fixed $1^\circ \times 1^\circ$ geographical grid cell (in which $1^\circ = 110.6$ km) was chosen because it is the approximate length of high-seas longlines (that is, 100 km long with an average of 1,200 baited hooks (Queiroz et al., 2016) that attract fish over long distances (Kroodsmas et al., 2018a; Kroodsmas et al., 2018b). In addition, the $1^\circ \times 1^\circ$ grid-cell size was suitable to reduce the effects of gaps in AIS coverage that, at smaller grid sizes, could potentially result in substantial unrecorded fishing effort per grid cell.

3.3.6 Ethical Consideration

The labeling procedures have been approved by the Marine Biological Association of the UK (MBA) Animal Welfare Ethical Review Body (AWERB) and licensed by the UK Home Office through staff and project licenses under the Animals (Scientific Procedures) Act 1986. Tagging procedures have been carried out under

Portuguese national laws for the use of vertebrate animals in research and the work and tagging protocol has been approved by the Azores Directorate of Marine Affairs of the Azores Autonomous Region (SRAM 20.23.02/Of.5322/ 2009), which monitors and approves scientific activities.

4. Results

4.1 Result One: Comparison between CMEMS and GLODAP data

4.1.1 CMEMS vs GLODAP Oxygen concentrations

To determine and compare the drift between model (CMEMS) and in-situ data from GLODAP, oxygen concentrations of CMEMS were linearly interpolated to obtain the oxygen concentrations at depths present in GLODAP. Vertical and oxygen gradient of both models from the sea surface to a depth of 2000 m meters (Fig 4.1, 4.2, 4.3) in 2011, 2017 and 2018 showed typical OMZ and non-OMZ waters.

In 2011, the oxygen gradient between both models in January differed, with CMEMS recording a minimum oxygen concentration of 6.2 ml/L at a depth of 100 m and GLODAP recording a minimum oxygen concentration of 4 ml/L at a depth of 300 m. In contrast, other months recorded minimum oxygen concentrations at an average depth of 700 m with an average oxygen concentration of 3.6 ml/L except for that which was recorded in November/December, with GLODAP recording the lowest at 2.5 ml/L. This was recorded in the OMZ of the ETA

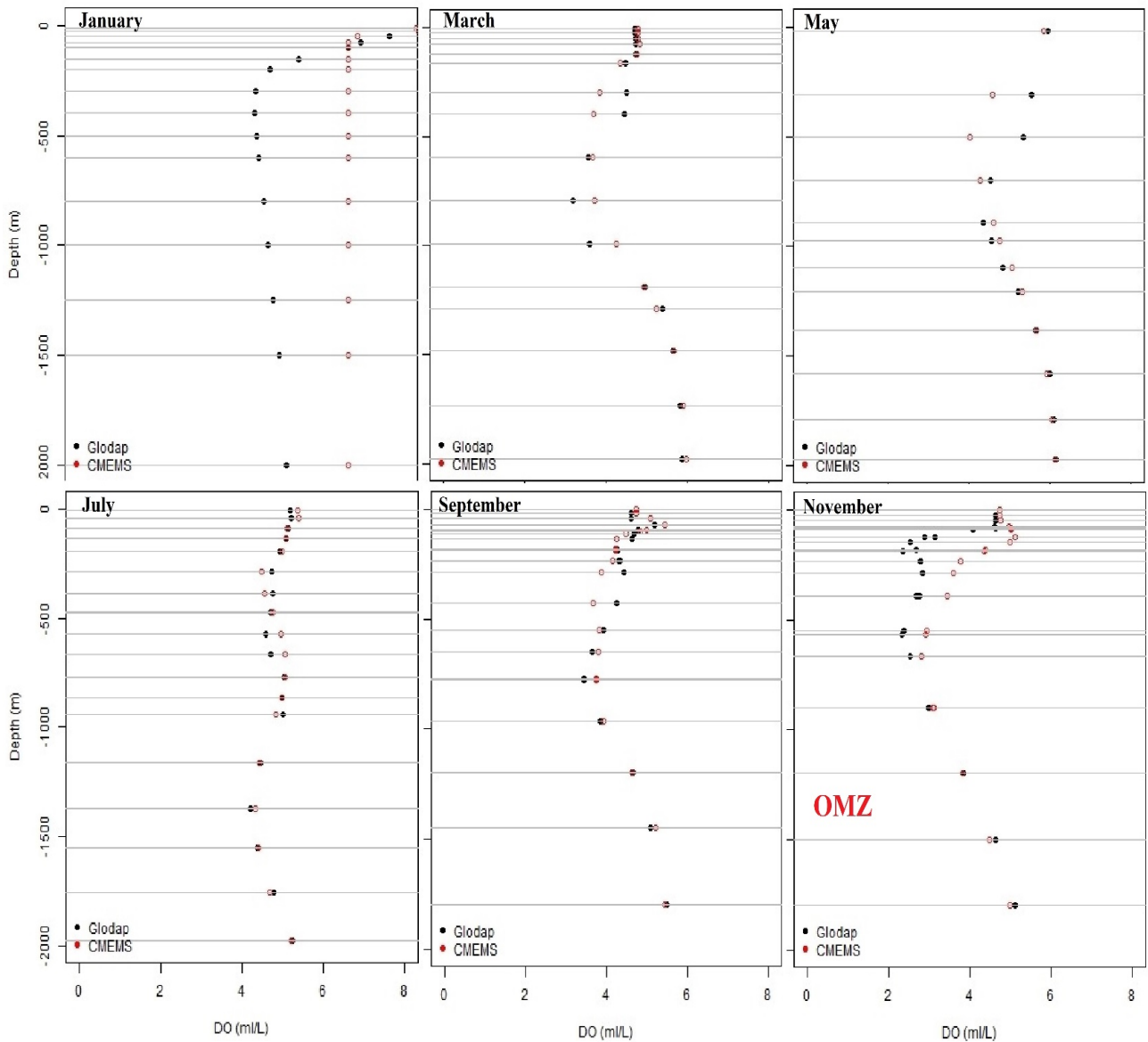


Figure 4. 1: Vertical gradient of oxygen concentration of CMEMS and GLODAP recorded in 2011

In 2017, oxygen concentrations of both models were observed to record the lowest in July/August and November/December, with a concentration of 1.6 ml/L and 2.3 ml/L, respectively, above a depth of 500 m in the OMZ.

GLODAP oxygen concentrations in March/April recorded a minimum of 3.0 ml/L at a depth of 800 m with an inverted oxygen concentration between GLODAP and CMEMS from 400 m to 1000 m. oxygen concentrations recorded in May/June followed the profile of a normoxia with a minimum oxygen concentration of 6ml/L. The oxygen concentrations of these two models for other months followed a similar pattern.

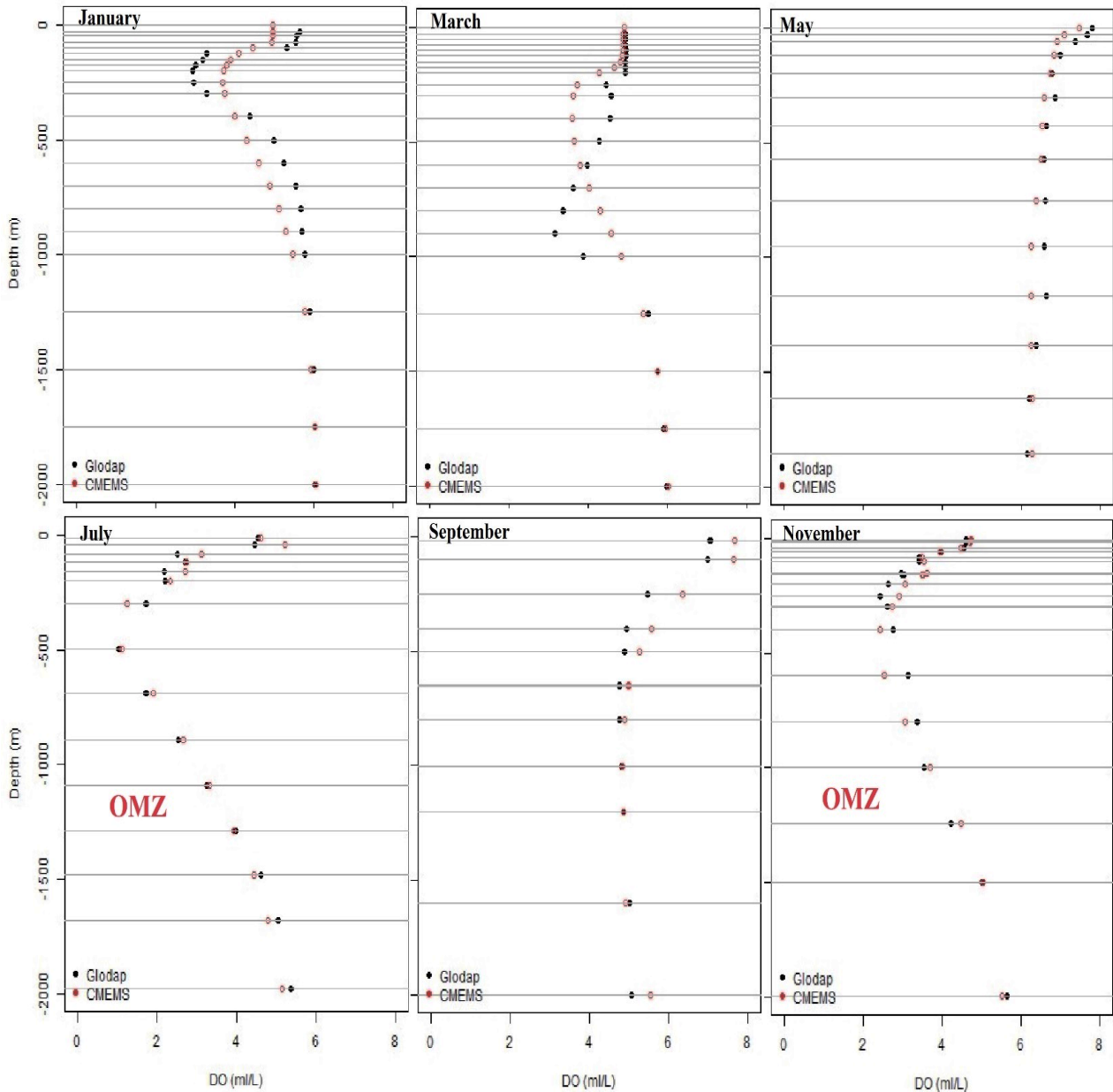


Figure 4. 2: Vertical gradient of oxygen concentration of CMEMS and GLODAP recorded in 2017

For all the months recorded in Fig 4.3, it was observed that the minimum oxygen concentrations in 2018 were generally above 500 m. In contrast to 2011, various months recorded different oxygen minimum concentrations, with the lowest concentration of 2.1 ml/L and 2.0 ml/L recorded for CMEMS and GLODAP, respectively, in May/June.

Minimum oxygen concentrations of 0.8 ml/L and 1.5 ml/L were recorded for CMEMS and GLODAP, respectively, in September/October, which was recorded in the OMZ of the Eastern Tropic Atlantic. This non-uniform pattern of oxygen concentrations can be attributed to the variation between model data and in-situ data, which were acquired through different methods and sensors.

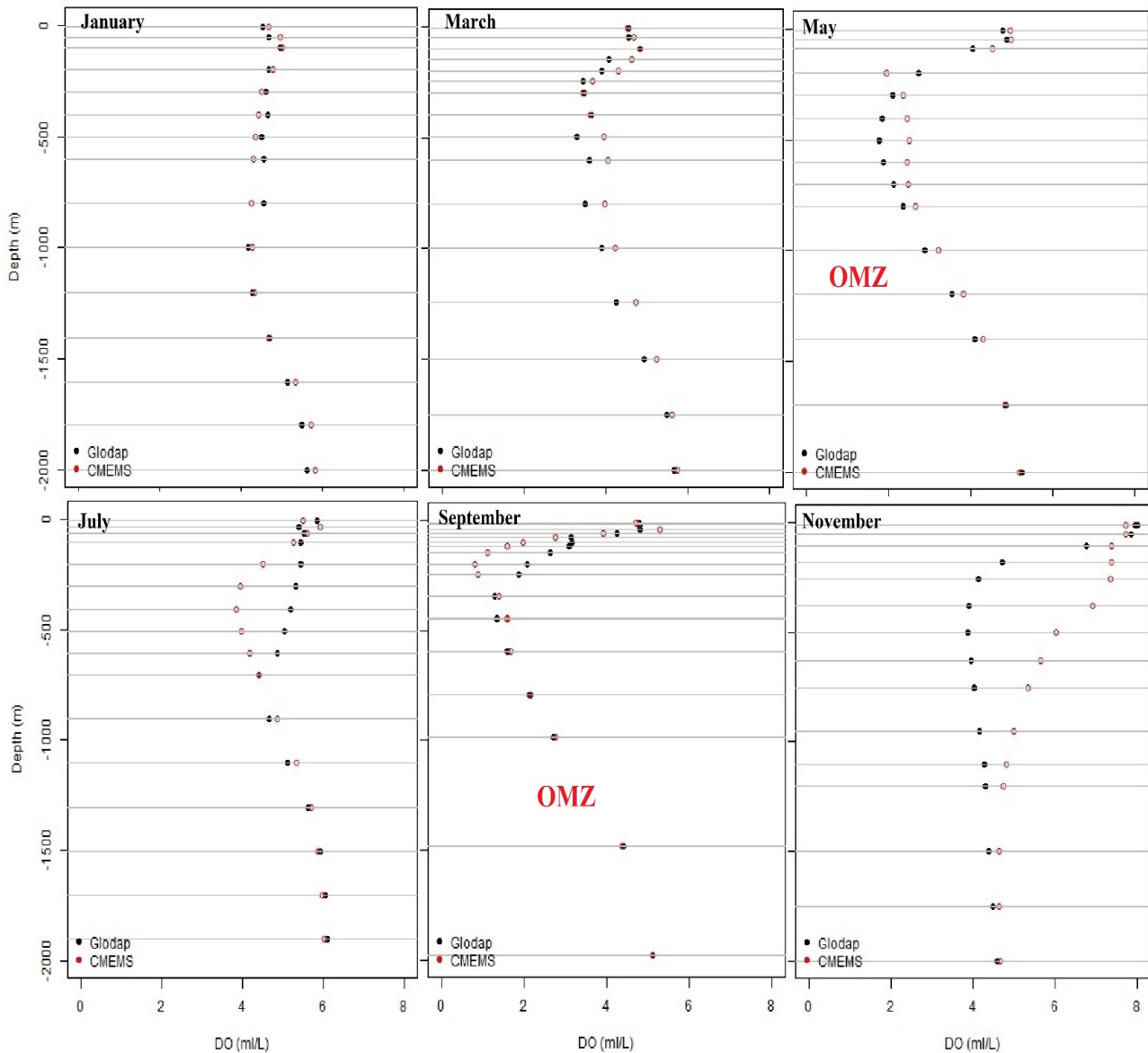


Figure 4. 3: Vertical gradient of oxygen concentration of CMEMS and GLODAP recorded in 2018

Statistical Variations in Oxygen concentrations

Subject to T-test statistical analysis, oxygen concentrations of CMEMS and GLODAP models were statistically different (p -value = 0.043) considering oxygen concentrations of sampled locations in both the North and South Atlantic oceans (Fig 3.1, section three). In contrast, variation in oxygen concentrations between GLODAP and CMEMS in the OMZs (i.e. study area) was statistically non-significant (p -value = 0.071). The significant difference in CMEMS and GLODAP in Fig 4.4A could be attributed to the large variations in oxygen concentration when considering oxygen concentrations both within and outside the OMZs.

Noteworthy, CMEMS and GLODAP data were acquired through different techniques. Since one is considering all sampled locations within the Atlantic Ocean,

large variations could be expected (the larger the area, the larger the variations between the oxygen concentrations of CMEMS and GLODAP). However, when sample locations were limited to the OMZs where the shark tracks were located in the North Central and ETA, i.e., 40° N, 0, 30° W, 0 oxygen gradients were consistent, and lower variation was observed. Also, variations in oxygen concentrations between GLODAP and CMEMS were non-significant (Fig 4.4B). Nonetheless, oxygen concentrations in both GLODAP and CMEMS were highly correlated, with a correlation value of 0.93 (Fig 4.5).

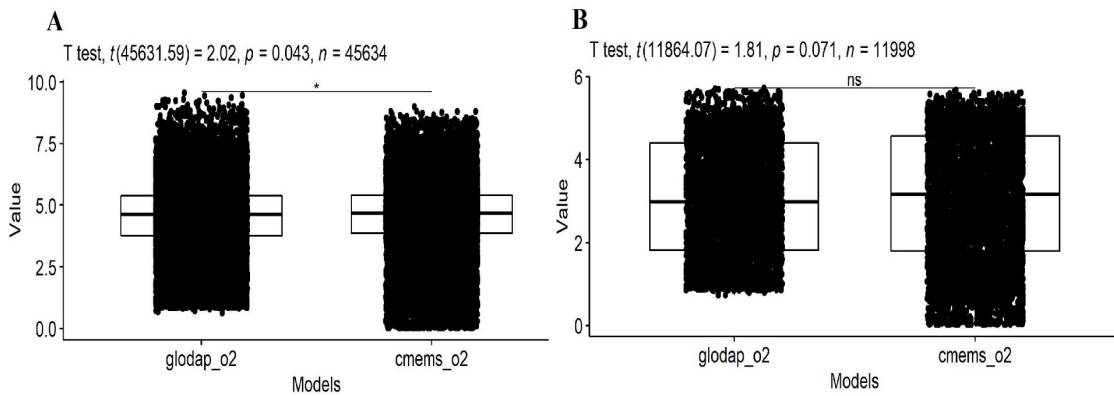


Figure 4. 4: Variation in oxygen concentrations between GLODAP and CMEMS in the (A) North/South Atlantic Ocean; (B) OMZs of ETA.

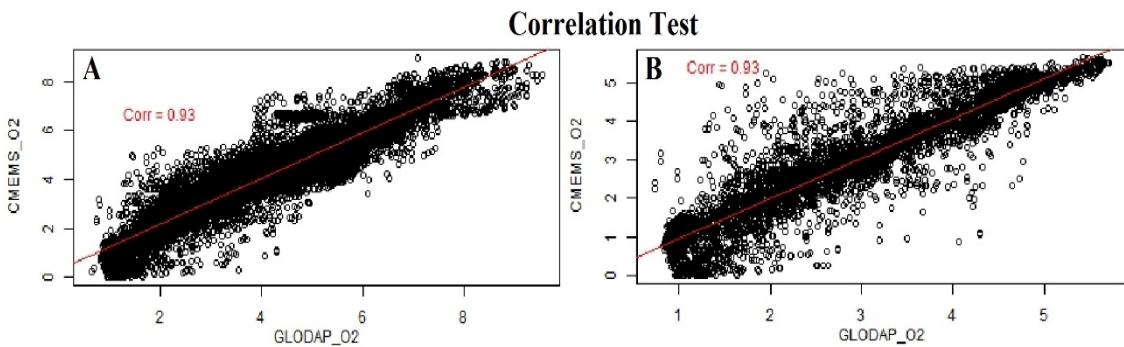


Figure 4. 5: Correlation test between GLODAP and CMEMS (A) North/South Atlantic Ocean (B) OMZs of ETA

To further validate the oxygen concentrations in CMEMS and GLODAP, the Root mean square error analysis of 0.55 obtained shows that CMEMS and GLODAP can accurately predict each with scatter component of the error (scatter index) of CMEMS and GLODAP in both scenarios below 20%. Still, values obtained for GLODAP indicate a good model performance over CMEMS by 0.04% which is less significant (Table 4.1). While the coefficient of determination (R²) of 0.87 and 0.86 in North & South Atlantic

Ocean and ETA OMZs, respectively, showed that over 80% variation in one model could be attributed to the variation in the other model.

Table 4. 1: Statistical summary of GLODAP vs CMEMS

Study Area	n	σ	RMSE	P-value	SI (%)		R ²
					GLODAP	CMEMS	
North and South Atlantic Ocean	45634	0.93	0.55	0.04	12.1	12.2	0.87
ETA OMZs	11998	0.93	0.56	0.07	18.5	18.8	0.86

$\alpha = 0.05^*$

4.2 Result Two: Identification and Characterization of Shark Foraging and Habitat Use in OMZ

4.2.1 Habitat Use

Fig 4.6A showed the kernel distribution of sharks with regards to their utilization distribution per grid cell. While it could be said that blue sharks have large aggregation close to their tag locations (Northwest of Cape Verde), the same could not be attributed to Mako sharks which were tagged in the same area. Due to their mobility and swimming agility, they could aggregate close to the west coast of Africa (Senegal, Mauritania, Western Sahara). In contrast, the shark occupancy in the number of days spent per grid cell (Fig 4.6B) was not in the same pattern as Fig 4.6A, probably because of the prey preferences of these two species. While the bulk of days spent in an area was concentrated in the north-western part of Cape Verde for blue sharks, the most days spent per grid cell was observed close to the shelf of Western Sahara. Where there was overlap/bias in Fig 4.6A and 4.6B, to ascertain the true distribution of the sharks per grid cell in the OMZs, the mean days the shark spent per grid cell (Fig 4.6C) compensated for this bias where all the tracks within a grid cell were summed and averaged by the total number of days spent within the grid cell. It, therefore, showed the true distribution in mean days the sharks spent per grid cell, and this was observed to be in the northwestern part of Cape Verde (Blue sharks) and shelf of Western Sahara (Mako shark).

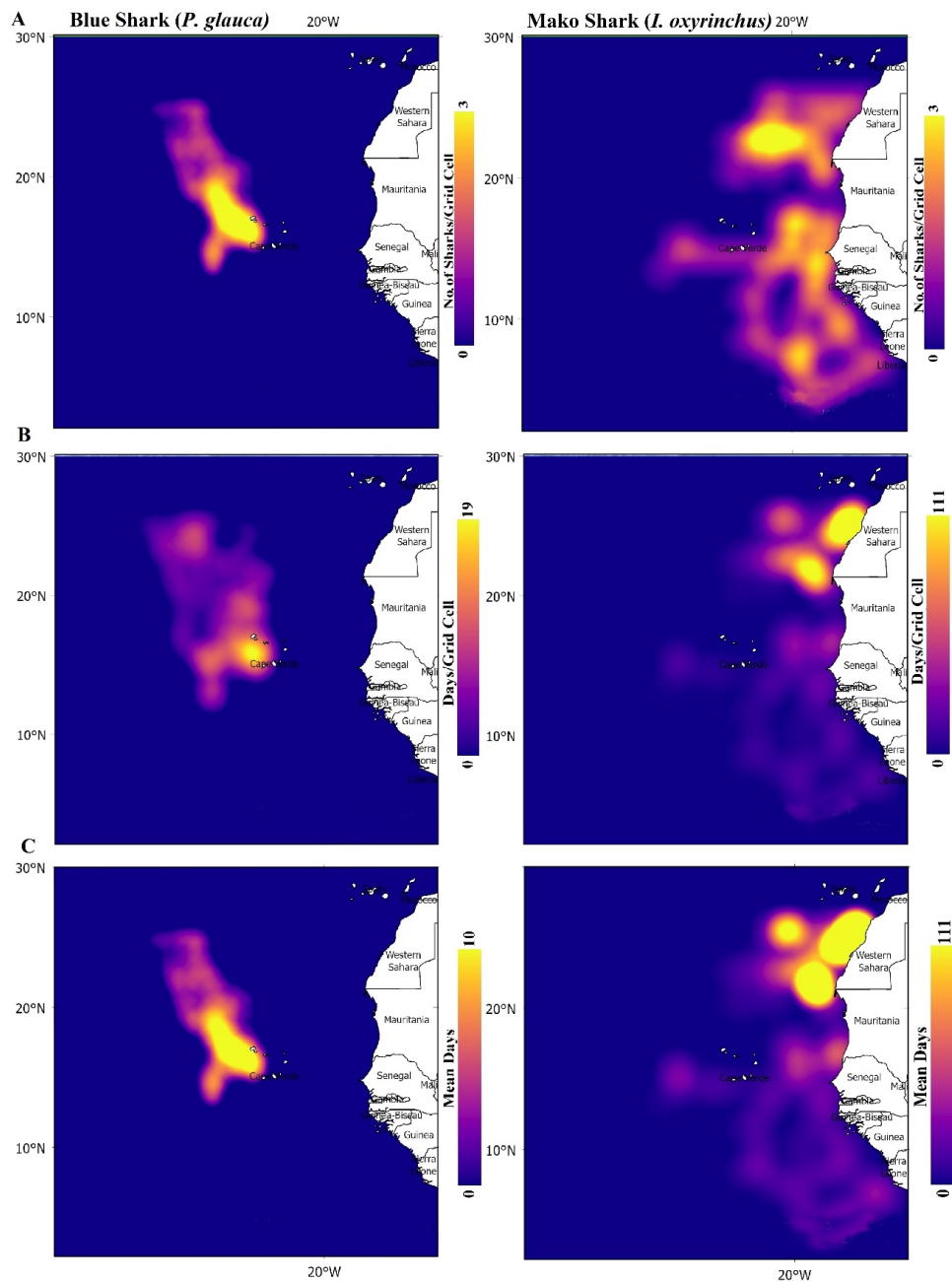


Figure 4. 6: Kernel density of utilization distribution from pooled geolocation tracks over study period. (A) Number of blue shark (left) and Mako sharks (right) per grid cell (B) Days blue shark (left) and Mako shark (right) spent per grid cell (C) Mean days spent per grid cell

4.2.1 Foraging and Environmental fields

Habit use of blue shark was at the OMZ fronts of Cape Verde (Fig 4.7A) and Fig 4.7B indicated OMZ front preference for shortfin mako shark at adjacent OMZ fronts of Western Saharan. Fig 4.7 revealed that the most time spent by the two species was neither outside nor inside the core OMZs but at the fronts. Perhaps, due to the high productivity of the area, they tend to spend more time where there was prey aggregation and often

dive less hypoxic waters and dive more in normoxia, reinforcing their habitat preference along the OMZ fronts.

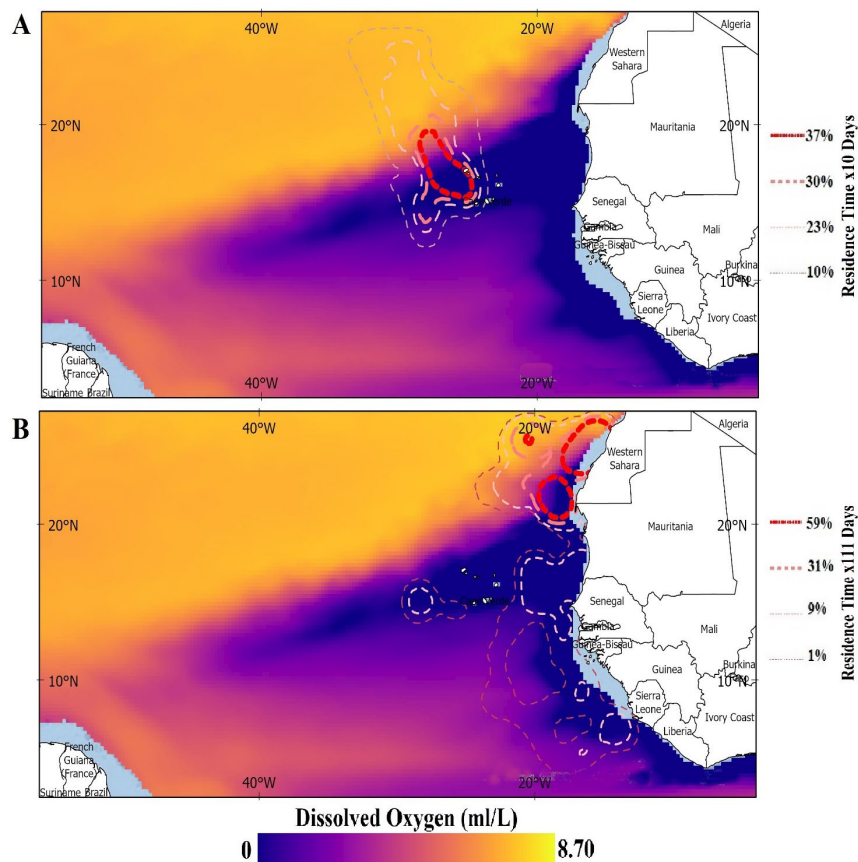


Figure 4. 7: Map of the study area in the North-east Atlantic. Three-year (2011, 2017, 2018) monthly average of dissolved oxygen at 100 m depth on the resident time (contour lines) of (A) Blue Sharks with residence time of 3 days (B) Mako sharks with mean residence time of 28 days

While there was no distinct correlation in Blue shark habitat use in Fig 4.8A and chlorophyll-a concentration, high chlorophyll concentration along the Western Sahara waters can be attributed to the cause of the high resident time of Mako sharks along the coast of West Africa and dominantly adjacent to the coast of Western Sahara. Chlorophyll concentration in seawater is a proxy for productivity, which often characterizes the preferred habitats of sharks (Queiroz et al., 2019).

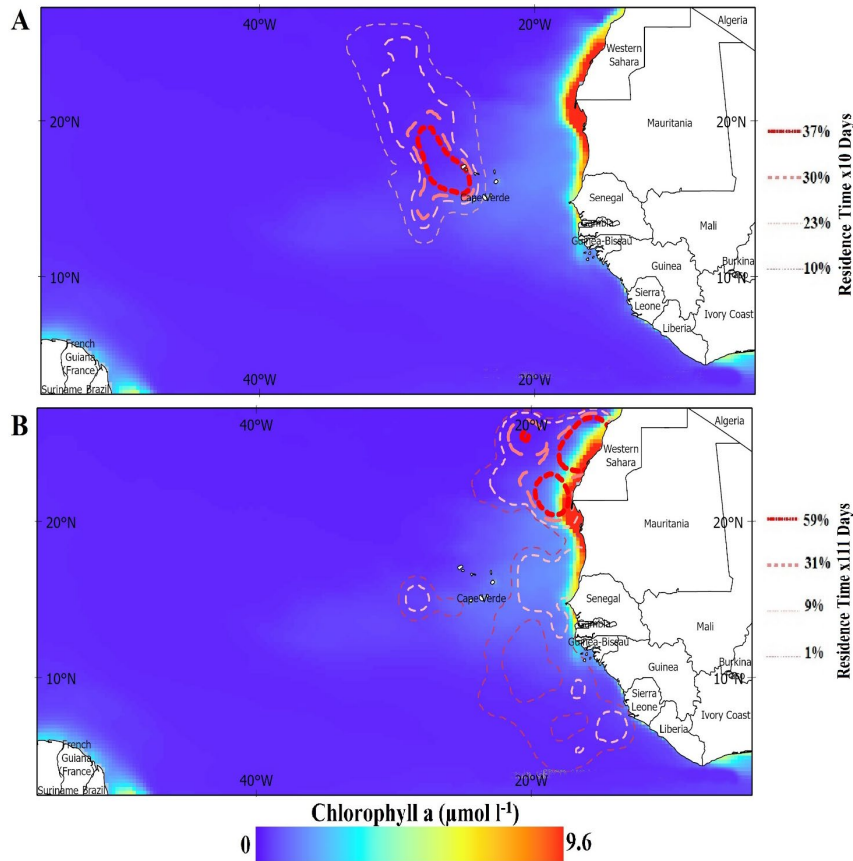


Figure 4. 8: Map of the study area in the North-east Atlantic. Three-year (2011, 2017, 2018) monthly average of Chlorophyll a on the resident time (contour lines) of (A) Blue Sharks with residence time of 3 days (B) Mako sharks. With mean residence time of 28 days

It was observed from Fig 4.9A that blue sharks largely occupy an area with high and low thermal gradient northwest of Cabo Verde while Mako sharks shown in Fig 4.9B occupied an area of high and low thermal contrast with an average temperature of 17°C.

Blue and Mako sharks preferred fronts with subsurface temperature gradients (fronts and thermoclines) and/or high primary productivity of Cabo Verde OMZ and Western Sahara OMZs, respectively.

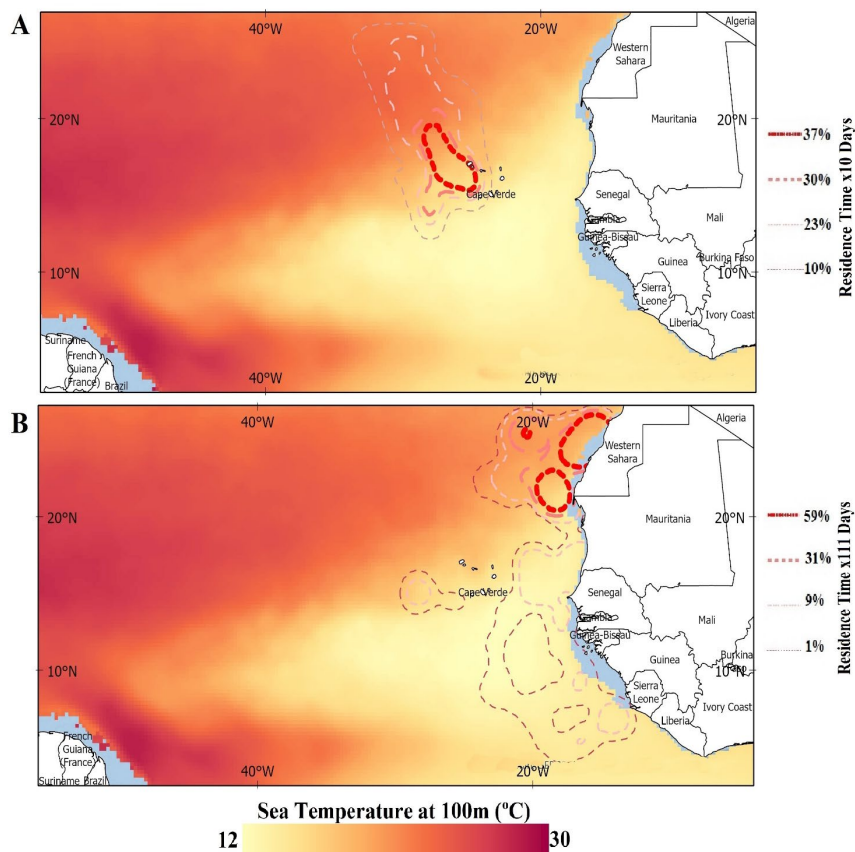


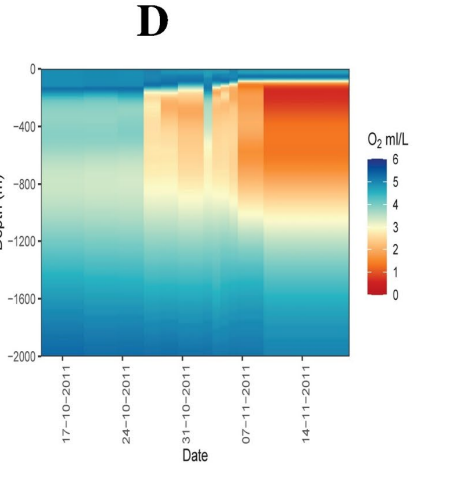
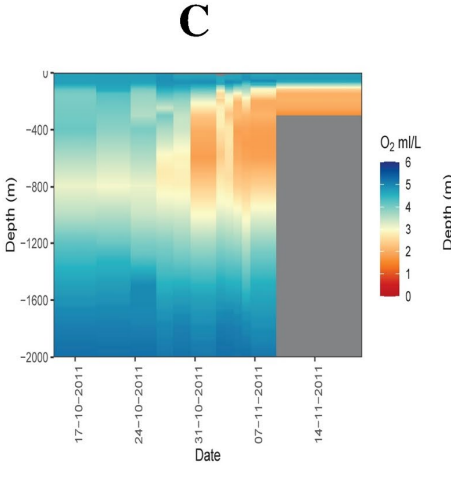
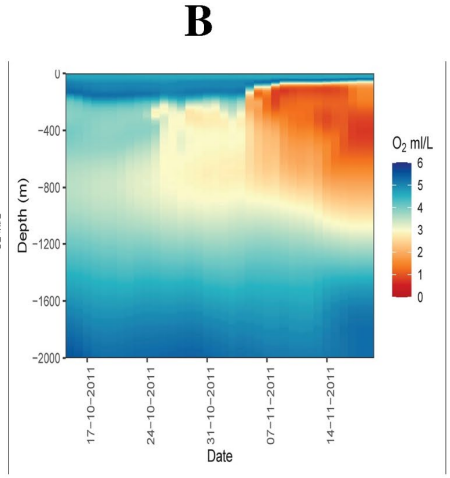
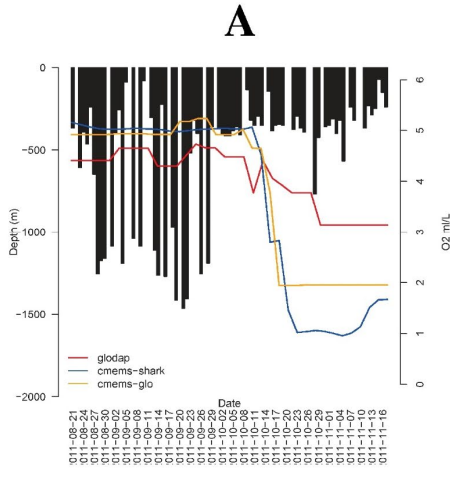
Figure 4. 9: Map of the study area in the North-east Atlantic. Three-year (2011, 2017, 2018) monthly average of sea temperature at 100 m on the resident time (contour lines) of (A) Blue Sharks with residence time of 3 days (B) Mako sharks with mean residence time of 28 days

4.3 Result Three: Hypoxia-Based Habitat Compression and Vulnerabilities to Fisheries

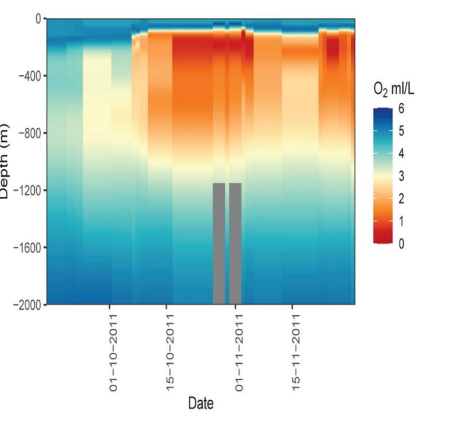
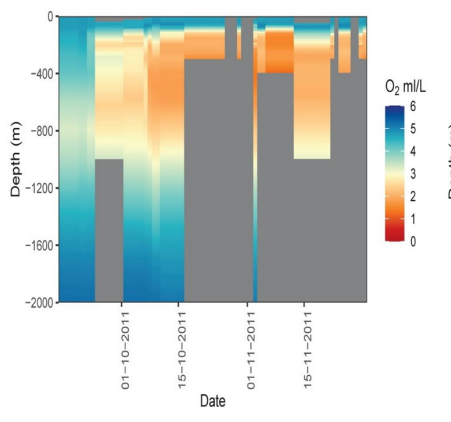
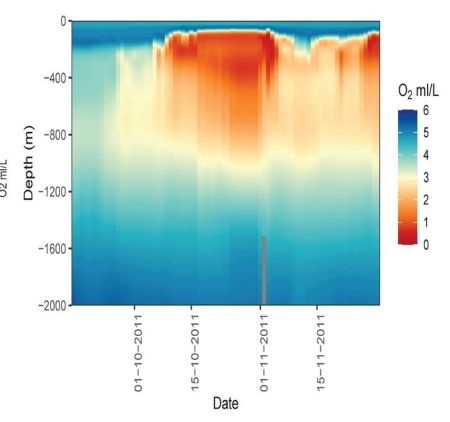
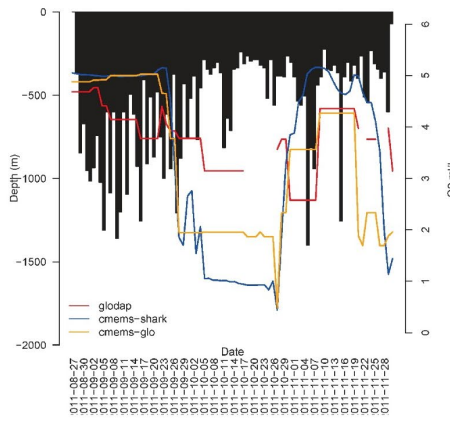
4.3.1 Oxygen Induced Habitat Compression and Shark behaviour

Dive pattern of blue sharks (bl_91026, bl_1070858, bl_164443 and bl_164444) shows consistency with the three models of DO concentrations. A maximum depth dive (MDD) of 1500 m was observed for bl_91026 with high DO, averaged 5 ml/L while the dive depth became shallow with decreasing DO concentration. The dissolved oxygen gradients from the surface to a depth of 2000 m were also observed for the three models for bl_91026 in Fig 4.10B-D. Alternating dives were observed for bl_7085, where dives between 500 m to 1400 m were observed at the beginning of the tracks, but during an encounter with adjacent waters with low DO concentration, the dive depth was limited to an average depth of 500 m for a brief period along the tracks while the dive increased to a depth of about 1400 m afterwards. For bl_164443, a vertical shift to shallower depths (increased shoaling) occurred as sharks moved across the core OMZ area compared to dive depths in adjacent waters where oxygen concentration was high. For example, the MDD depths of bl_164443 in adjacent waters to the OMZ ranged between 400 and 1500

m, whereas above the core OMZ area, MDD depths were 200– 650 m (Fig 4.10). However, while MDD of bl_164444 reached 1600 m in water with high DO, shallow dives (200-500 m) were recorded in the adjacent waters along its tracks. This was also observed in the OMZ, where DO was low and yet, deep intermittent dives averaged 1200 m.



bl_91026



bl_107085

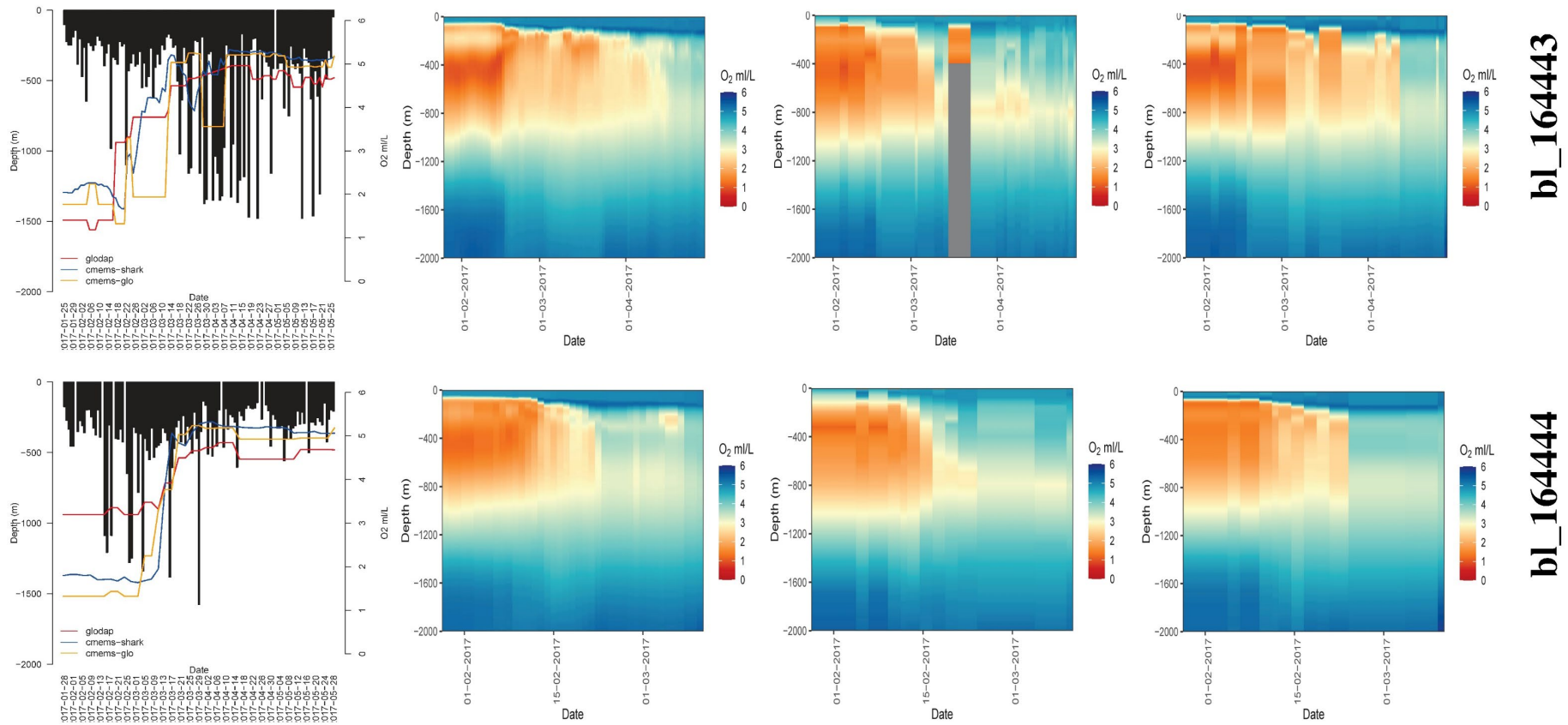
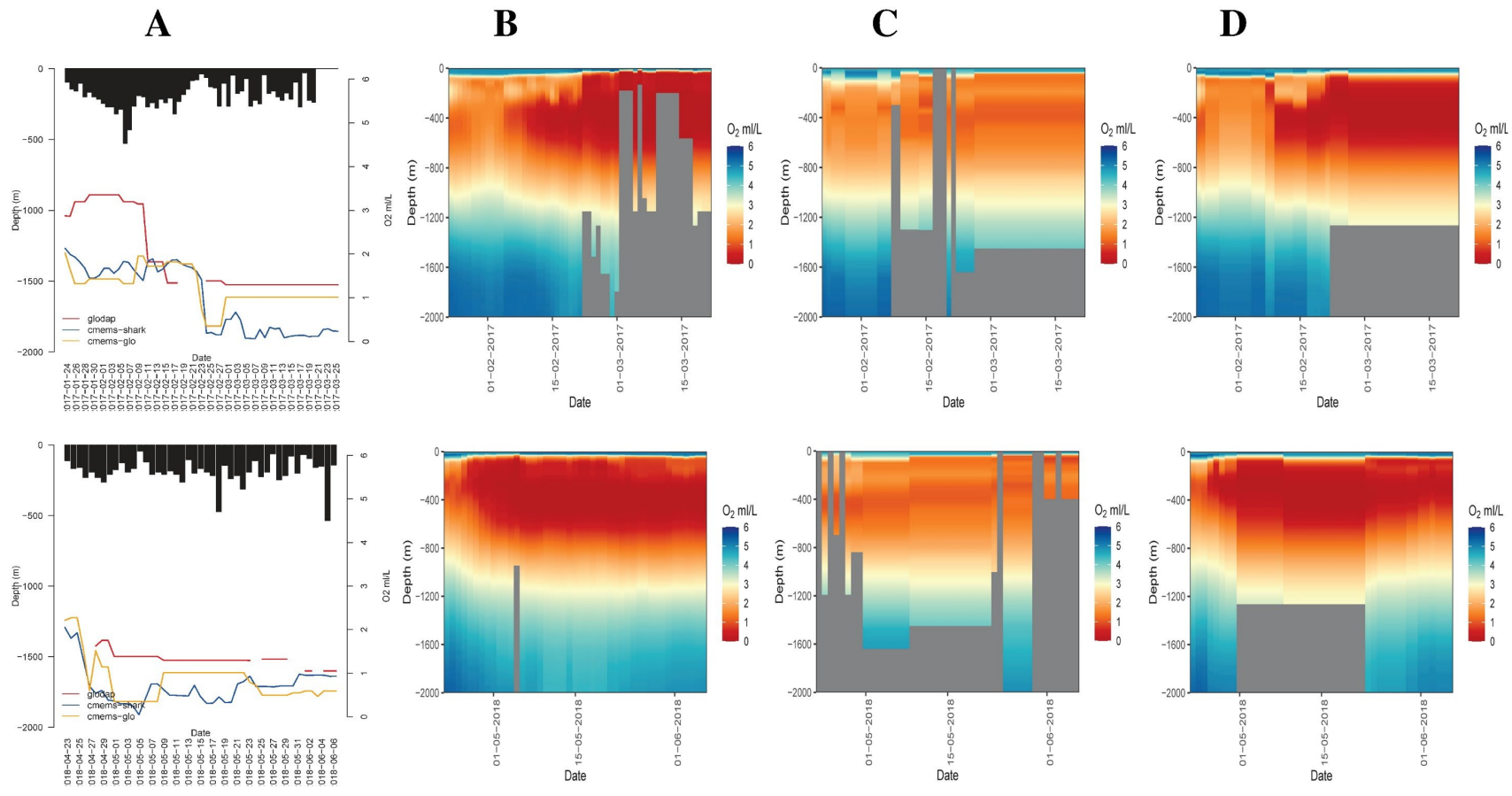


Figure 4. 10: Dive response of blue sharks to oxygen concentration (A) Vertical movement of Blue sharks in relation to dissolved oxygen models. Daily maximum depth plots (black) for blue shark overlaid on GLODAP (red), CMEMS (yellow), and GLODAP-CMEMS (blue) DO concentration data at 100 m [see legend] (B) CMEMS DO concentration from the surface to 2000 m during shark movement (C) GLODAP DO concentration from the surface to 2000 m during shark movement. The dark grey area corresponds to where no data was available (D) CMEMS-GLODAP DO concentration from the surface to 2000 m during shark movement.

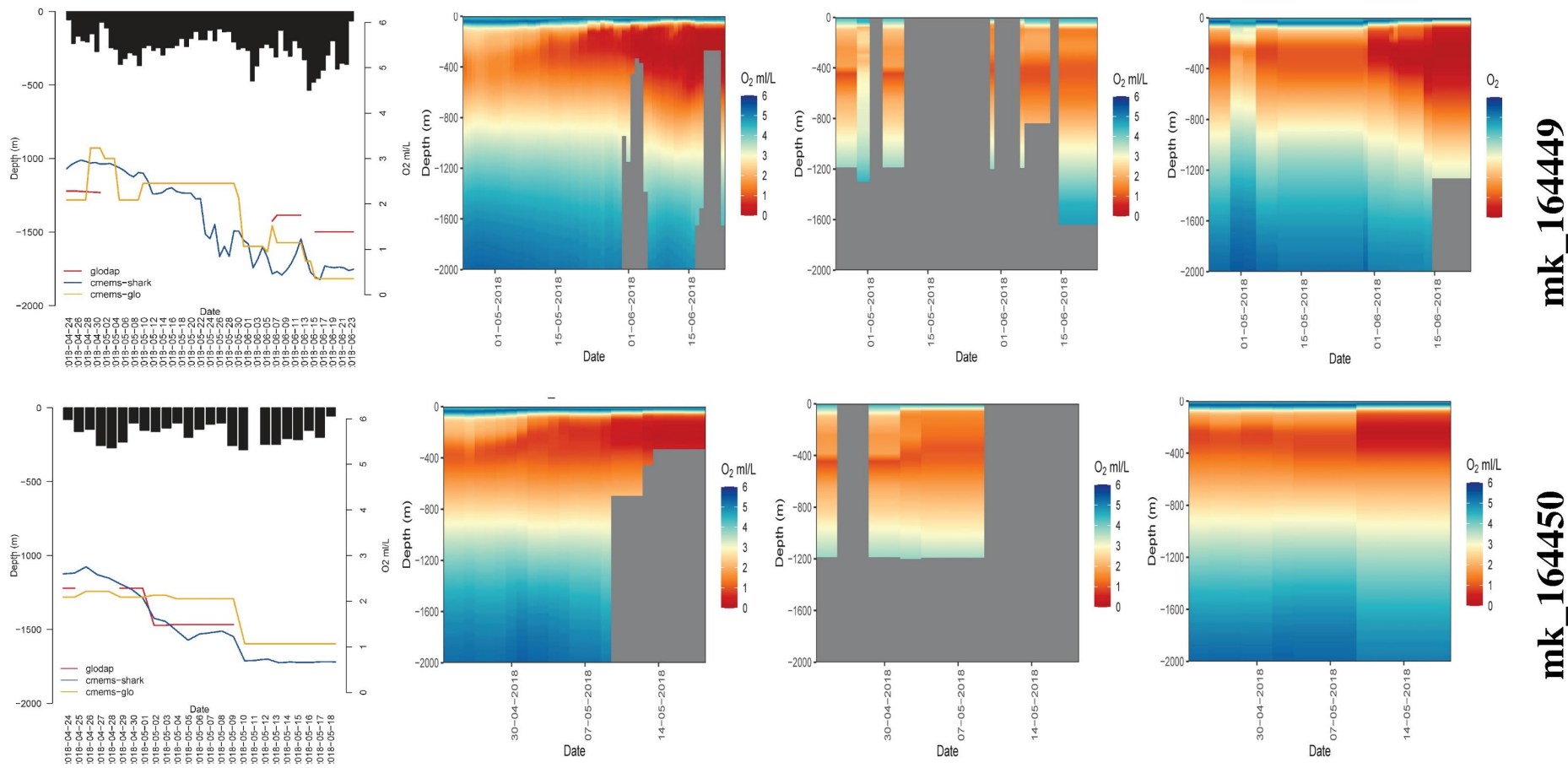
Oxygen concentrations encountered by each shark for the three oxygen datasets follow the same colour pattern (which corresponds to oxygen concentrations) with an oxygen minimum zone (<3.5 ml/l) varying between 100 m – 1000 m. 1 and 2 with high oxygen concentration across all depth from the start of shark movement in normoxia to OMZ area, 3 and 4 were from the core OMZ to the normoxia in which 3 spent longer duration across the OMZ.

For all Mako sharks (mk_164446, mk_164448, mk_164449 and mk_164450) in Fig 4.11 that encountered OMZ with an average DO concentration of 2 ml/L, an average MDD of 300 m was recorded, while the MDD recorded was at 550 m for all the four sharks. This was in contrast to the dive depth of blue sharks (Fig 4.10) with higher MDDs.



mk_164446

mk_164448



mk_164449

mk_164450

Figure 4. 11: Dive response of Mako sharks to oxygen concentration (A) Vertical movement of blue sharks in relation to dissolved oxygen models. Daily maximum depth plots (black) for blue shark overlaid on GLODAP (red), CMEMS (yellow), and GLODAP-CMEMS (blue) DO concentration data [see legend] (B) CMEMS DO concentration from the surface to 200 m during shark movement (C) GLODAP DO concentration from the surface to 200 m during shark movement (D) CMEMS-GLODAP DO concentration from the surface to 200 m during shark movement.

A consistent oxygen concentrations pattern can be observed across the plotted three oxygen concentration datasets with low oxygen concentration (<3.5 ml/l) varying between 100 m to 1000 m

4.3.2 Shark's Vulnerabilities to Fisheries

The extent of spatial overlap between the relative density distribution of sharks and longline-fishing efforts indicates which species are more at risk from fishing and how this risk is distributed. Fig 4.12 showed the mean monthly distribution of fishing effort (mean days per grid cell) of AIS-tracked longline fishing vessels in 2012–2020 and the percentage of mean days per grid cell in overlapped areas for blue (Fig 4.12A) and Mako sharks (Fig 4.12B) in the North Atlantic Ocean in 2011, 2017 and 2018. It was observed that the spatial use and density of Mako sharks (59%) are more susceptible to fisheries. Also, the hotspot is known for its upwelling and high productivity aggregate of many pelagic sharks, which are ultimately susceptible to longline fishing vessels in the area. In contrast, blue sharks' spatial use of northwest Cape Verde with no fishing hotspot makes the blue sharks less susceptible to commercial fishing. Because the large proportion of shark mortality related to fishing (Queiroz et al., 2019) is related to longline-fishing efforts in areas of shark space use, it follows that sharks that have both a high overlap with fishing effort (greater susceptibility) will be at a greater risk of capture than those with low overlap.

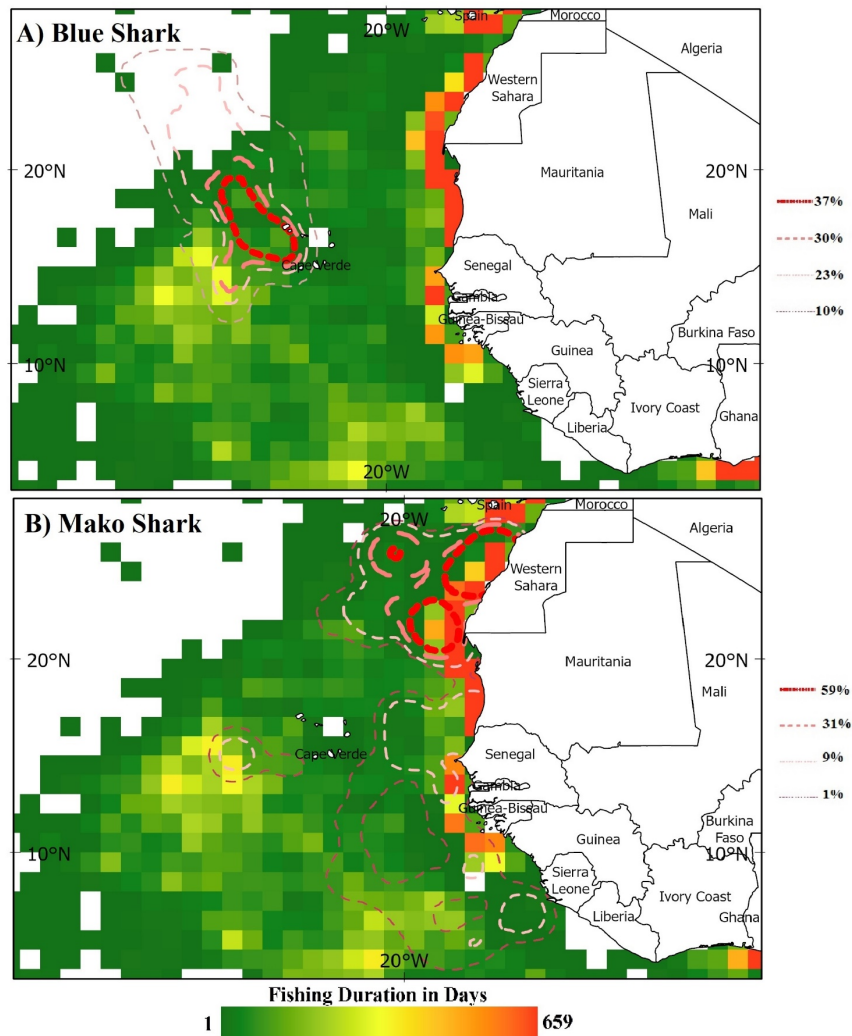


Figure 4. 12: Spatial distributions and overlap of sharks and longline fishing vessels. Distribution of the mean monthly overlap and the level of fishing effort (in days) that sharks were exposed to in overlapping areas for all species within $1^\circ \times 1^\circ$ grid cells (A) Percentage density of exposure of blue sharks in $1^\circ \times 1^\circ$ grid cells (B) Percentage density of exposure of blue sharks in $1^\circ \times 1^\circ$ grid cells

5. Discussion

Results from the comparison between CMEMS and GLODAP showed the reliability of both models. Even though Copernicus Services relies on several environmental measurements collected by data providers external to Copernicus (i.e. from ground-based, sea-borne or air-borne monitoring systems, geospatial reference or ancillary data), oxygen concentrations in CMEMS and GLODAP were similar with a standard deviation of ± 1.51 . This is low when acceptable considering the volume of data of GLODAP data points which was matched with CMEMS across the Atlantic Ocean. Low statistical variations within the OMZs can be attributed to the relatively uniform oxygen concentration at depth commonly experienced in the OMZs due to its high stratification. OMZ observed from the two models ranges from a depth of 200 – 1000 m in the ETA. This was reported in previous studies by Stramma et al. (2012), and Keeling et al. (2010) on the expansion of the OMZ as the global decline in ocean oxygen levels will alter the headwaters aerating the OMZs within the water column.

Tiano et al. (2014) stated that the centre of the ETA is practically anoxic, with oxygen concentrations within the OMZ core found to be $< 0.1 \mu\text{mol kg}^{-1}$ between depths of 150 and 800 m which corroborates our result of extremely low DO concentration in the OMZ. Helly and Levin (2004) reported a thickness of eastern tropical pacific OMZs of between 200-1200 m which was observed in Fig 4.1, 4.2 and 4.3, and this influences population dynamics along the continental margin. Results showed the differences between the vertical gradients of oxygen concentration in the core OMZ and outside the OMZ. While the oxygen field from both models was subjected to a correlation test, it was strongly correlated with a value of 0.93. A root means square of less than 20% was indicative of one model being able to predict the other. There was a non-significant variation in the oxygen field of both models within the OMZ. In contrast, there was a significant test in oxygen concentration from both models when the Atlantic Ocean was considered as a study area with more data points and heterogeneous characteristics.

Habitat preferences of Blue and Mako sharks are subjective. While the kernel density of utilization distribution of these sharks in mean days (Fig 4.6c) revealed their habitat preference, this could also be attributed to foraging sites where prey is abundant, with a strong correlation between fishing density (hotspot) and Prey aggregation affecting their choice of foraging habitat (Fig 4.12). Reasons for this habitat preference and distribution could also be related to larger-scale movements associated with new

foraging opportunities, namely the availability of certain prey species at greater depths (Clarke & Stevens 1974) or in response to local oceanographic conditions (e.g. surface water temperatures). However, shark birthing and mating activities have also been associated with such movements (Weng et al., 2005, 2007).

Concerning optimal foraging theory, predators should maximize the time they spend in a prey bed. Therefore, the fact that recorded Mako sharks (Fig 4.6c) remained in the fishing hotspots around and off the coast of Western Sahara could indicate successful foraging in this area. Nonetheless, this horizontal shift in horizontal and/or depth distribution could also be associated with a change in prey type as sharks move from coastal to open water habitats.

Previous studies show that the stomach contents of blue sharks caught in the English Channel consisted mainly of schooling epipelagic fish (Stevens 1973), while blue sharks in the Bay of Biscay fed mainly on squid species most likely found in deep water (Clarke & Stevens 1974).

A strong relationship between some environmental variables occurs in sharks' horizontal and vertical movement. While sharks prefer fronts with high thermal gradients (Fig 4.9), they also exhibit this horizontal movement with oxygen concentration (Fig 4.7), just as they do with their diving pattern in hypoxic and normoxia waters. Queiroz et al. (2012) found a high correlation between shark habitat use and chlorophyll concentration, as these areas are known for their high productivity as in the coastal waters of Western Sahara (Fig 2.8b), hence their aggregation in this area. A correlation between whale shark distribution and proximity to the shelf margin has been described for the northern Gulf of Mexico and may be related to productivity surges associated with these areas (Gonzalez-Quiros et al., 2003). The dynamic physical processes associated with shelf margins produce an upwelling of nutrient-rich water to the surface (Huthnance, 1981), resulting in a localized increase in planktonic biomass.

Oxygen plays a key role in the diving pattern and habitat preference of Blue and Mako sharks vertically and horizontally. This became clear in Fig 4.10, as different oxygen concentration gradients significantly influenced the diving behaviour of blue sharks. Vedor et al. (2021) suggested that blue sharks' reduced maximum diving depths and lower frequency of deep diving were caused by sharp horizontal and vertical gradients in the physical and biological variables present in the OMZ. Different driving patterns could also indicate different activities and behaviours of the sharks. While blue sharks tend to dive deeper than Mako sharks (Fig 4.11), they exhibit a U- or V-shaped

dive during ascent or descent, with U-shaped dives associated with foraging on aggregated patches of prey at depth (Queiroz et al., 2017). This interpretation is widely supported by theoretical expectations and empirical results from previous studies. V-shaped dives of short duration at depth are believed to correspond to exploratory or transitional behaviour (Wilson and Block, 2009; Horodysky et al., 2007).

It is possible that by swimming up and down through the water column and traversing different depth layers; sharks increase the likelihood of detecting olfactory cues since scent trails in the ocean propagate in a horizontal plane due to current shear between different dense layers (Carey and Scharold, 1990; Pade et al., 2009). In addition, an examination of vertical movements reveals two distinct patterns that appear to be related to phases of offshore residency or migration. The first is characterized by oscillating driving behaviour, and the second is by a bimodal depth distribution with significant surface time (Nasby-Lucas et al., 2009). Using vertical movement to distinguish between possible foraging and migratory behaviours will dramatically improve efforts to use state-space models to quantify behavioural modes (Josen et al., 2007; Patterson et al., 2008; Bailey et al., 2008).

Fig 4.11 shows the general shallow diving depth of the shortfin mako, which are known to spend 90% of their time at night at depths less than 100 m, while during the day, they spend 76% at this depth zone (Stevens et al., 2010). Acoustic telemetry studies of juvenile shortfin mako fish off southern California indicate that they spend about 80% of their time in surface waters less than 12 m deep and that excursions to deeper, cooler water are more common during the day. These studies show that although they seek out the upper mixed layer, they often make vertical oscillations and that larger sharks swim to greater depths than smaller individuals (Holts and Bedford, 1993; Klimley et al., 2002; Sepulveda et al., 2004). A large shortfin mako recorded in the northwest Atlantic spent most of its time well below the mixed layer, reaching depths of more than 400 m (Carey and Scharold 1990). The juvenile sharks off southern California spent about 82% of their time at 20–21°C and another 11% at 18–20°C (Holts and Bedford 1993). The blue sharks tagged in this study spent a lot of time in the tag area (northwest of Cape Verde), while the shortfin mako sharks spent more time outside the tag area and more time in Western Sahara waters.

The result from Fig 4.12 showed the spatial overlap and vulnerability of Mako sharks to fisheries which was not the case for blue sharks, as the spatial use does not overlap with known commercial fisheries (Kroodsma et al., 2018b). Considering the high

fishing effort in hotspots of Mako shark space exploitation for much of the year and the very few spotted hotspots that are free of exploitation, it became clear that the risk of shark exposure from fishing in Western Sahara is high spatially is extensive, this risk of exposure extends almost across the entire shelf. Since this area is known for its high productivity (Fig 4.8), the observed patterns point to a future in which sharks find limited spatial sanctuary from industrial longline fisheries. More worrisome is that they are currently concentrated on ecologically important hotspots of space exploitation for the oceanic sharks unless they move south, which could overlap with the Senegalese fishing hotspot along the West African coastal corridor. Queiroz et al. (2019) highlighted the scale of the overlap between fishing efforts and hotspots of space used by sharks. They argued for more effective and timely monitoring, reporting and management of pelagic sharks.

Furthermore, to enhance the recovery of vulnerable species, one solution is to design large-scale marine protected areas around ecologically important space-use hotspots of pelagic sharks (Scales et al., 2014). Studies have shown that longline fishing patterns above the ETA OMZ form among the most important fishing hotspots within the entire eastern Atlantic, particularly along with the northern extent of the ETA OMZ (Vedor et al., 2021) with a high correlation between high productivity and fishing effort hotspots. Consequently, vessels above the OMZ deploy longlines continuously (daily) continuously in localized areas rather than interrupt fishing by travelling for days between fishing hotspots (Queiroz et al., 2016).

6. Conclusion

To fully resolve the behavioural and foraging pattern of sharks across the OMZs, all-important environmental variables must be integrated. While previous studies showed that blue sharks probably have the most extensive horizontal coverage, they also have one of the deepest dives. However, during these extensive movements, they encounter a wide range of water with different characteristics, but the movement pattern changes while in the OMZs, where they dive 40% less in the ETA OMZ compared to adjacent waters with normoxia (Vedor et al., 2021). Although Mako sharks recorded an average MDD of 300 m, their spatial and horizontal coverage was more than the blue sharks. Blue and Mako sharks will experience further habitat compression to the uppermost 100 m of the water column in the OMZ areas to avoid or compensate for the low oxygen concentration at lower depth, potentially exposing them to fisheries, as this study has shown in the case of Mako sharks. This compression can also be associated with the physiological limits of sharks (Payne et al., 2015; Coffey et al., 2017; Sims, 2019), habitat compression of prey species (Gilly et al., 2013; Childress and Seibel, 1998) or even visual impairment caused by hypoxia (McCormick and Levin, 2017).

The results of this study support the hypothesis that a change in feeding patterns and increased aggregation of pelagic sharks in the OMZs is directly linked to the productivity of the areas, as in the case of the adjacent waters of Western Sahara, which could make them vulnerable to fishing. Time series data of all environmental variables (in-situ and modelled data) can be fully integrated with shark data to access even higher spatial and temporal resolution of shark behaviour and foraging in the OMZs. Recent technological advances in using archival satellite tags to measure dissolved oxygen concentrations in situ in conjunction with modelled and time-series data from cruise ships in the shark-occupied natural environment (Coffey and Holland, 2015) have proven to be extremely informative in determining the environment Niche of the species. Considering the environmental and physiological data from an ecological framework has helped to understand how interactions between species and food web dynamics, including the abundance of predators and prey, are affected.

As the global status of blue and shortfin mako sharks continues to decline, it is imperative to begin implementing conservation and management measures at offshore shark space exploitation hotspots, with simultaneous satellite monitoring of megafauna and fishermen as a tool for near real-time, dynamic management. Given the usefulness of oxygen for determining climate change impacts on marine ecosystems and for a better

understanding of ecological interactions in the ocean, further studies which would capture the routine and continuous recording of its concentration regarding these top marine predators will be particularly relevant and promising.

References

- Abascal, F. J., Quintans, M., Ramos-Cartelle, A., & Mejuto, J. (2011). Movements and environmental preferences of the Shortfin Mako, *Isurus oxyrinchus*, in the southeastern Pacific Ocean. *Marine Biology*, 158(5), 1175–1184. <https://doi.org/10.1007/s00227-011-1639-1>
- Al Azhar, M., Lachkar, Z., Lévy, M., & Smith, S. (2017). Oxygen Minimum Zone Contrasts Between the Arabian Sea and the Bay of Bengal Implied by Differences in Remineralization Depth. *Geophysical Research Letters*, 44(21), 11,106–11,114. <https://doi.org/10.1002/2017GL075157>
- Ardizzone, D., Cailliet, G. M., Natanson, L. J., Andrews, A. H., Kerr, L. A. and Brown, T. A. (2006) Application of bomb radiocarbon chronologies to Shortfin Mako (*Isurus oxyrinchus*) age validation. *Environmental Biology of Fishes* 77, 355–366.
- Bailey H, Shillinger G, Palacios D, Bograd S, Spotila J, et al. (2008) Identifying and comparing phases of movement by leatherback turtles using state-space models. *J Exp Mar Biol Ecol* 356: 128–135
- Bakun A, Field DB, Redondo R.A, Weeks SJ. (2010). Greenhouse gas, upwelling favorable winds, and the future of coastal ocean upwelling ecosystems. *Glob. Change Biol.* 16:1213–28
- Banse, K., (1968.) Hydrography of the Arabian Sea shelf of India and Pakistan and effects on demersal fishes. *Deep Sea Res. Oceanogr. Abstr.* 15, 45–48.
- Baum, J. K. and Myers, R. A. (2004) Shifting baselines and the decline of pelagic sharks in the Gulf of Mexico. *Ecology Letters* 7, 135–145
- Baum, J. K., Myers, R. A., Kehler, D. G., Worm, B., Harley, S. J., & Doherty, P. A. (2003). Collapse and conservation of shark populations in the Northwest Atlantic. *Science*, 299(5605), 389–392. <https://doi.org/10.1126/science.1079777>
- Behrenfeld MJ, O'Malley RT, Siegel DA, McClain CR, Sarmiento JL, (2006). Climate driven trends in contemporary ocean productivity. *Nature* 444:752–55
- Beman JM, Popp BN, Alford SE. 2012). Quantification of ammonia oxidation rates and ammonia oxidizing archaea and bacteria at high resolution in the Gulf of California and eastern tropical North Pacific Ocean. *Limnol. Oceanogr.* 57:711–26
- Bograd SJ, Castro CG, DiLorenzo E, Palacios DM, Bailey H (2008). Oxygen declines and the shoaling of the hypoxic boundary in the California Current. *Geophys. Res. Lett.* 35: L12607
- Bond, M. E., Tolentino, E., Mangubhai, S., & Howey, L. A. (2015). Vertical and horizontal movements of a silvertip shark (*Carcharhinus albimarginatus*) in the Fijian archipelago. *Animal Biotelemetry*, 3(1), 1–7. <https://doi.org/10.1186/s40317-015-0055-6>
- Bopp, L., Le Quéré, C., Heimann, M., Manning, A. C., and Monfray, P (2002). Climate-induced oceanic oxygen fluxes: Implications for the contemporary carbon budget, *Global Biogeochemical Cycles*, 16, 1-13.
- Brandt, P., Bange, H. W., Banyte, D., Dengler, M., Didwischus, S. H., Fischer, T., Greatbatch, R. J., Hahn, J., Kanzow, T., Karstensen, J., Krortzinger, A., Krahnemann, G., Schmidtko, S., Stramma, L., Tanhua, T., and Visbeck, M. (2015): On the role of circulation and mixing in the ventilation of oxygen minimum zones with a focus on the eastern tropical North Atlantic. *Biogeosciences*, 12, 489-512.
- Brauner, C.J., Randall, D.J., (1998). The linkage between oxygen and carbon dioxide transport. In: Perry, S.F., Tufts, B. (Eds.), *Fish Physiology. Fish Respiration*, 17. *Academic Press*, New York, pp. 283–319.

- Breitburg, D., (2002). Effects of hypoxia, and the balance between hypoxia and enrichment, on coastal fishes and fisheries. *Estuaries* 25 (4B), 767–781.
- Breitburg, D., Levin, L. A., Oschlies, A., Gregoire, M., Chavez, F. P., Conley, D. J., Garcon, V., Gilbert, D., Gutierrez, D., Isensee, K., Jacinto, G. S., Limburg, K. E., Montes, I., Naqvi, S. W. A., Pitcher, G. C., Rabalais, N. N., Roman, M. R., Rose, K. A., Seibel, B. A., Telszewski, M., Yasuhara, M., and Zhang, J (2018). Declining oxygen in the global ocean and coastal waters. *Science*, 359.
- Bunn, H.F., Poyton, R.O., (1996). Oxygen sensing and molecular adaptation to hypoxia. *Physiol. Rev.* 76, 839–885.
- Cailliet, G. M., Martin, L. K., Harvey, J. T., Kusher, D. and Welden, B. A. (1983) Preliminary studies on the age and growth of blue, *Prionace glauca*, common thresher, *Alopias vulpinus*, and short-fin mako, *Isurus oxyrinchus*, sharks from California waters. In: Proceedings of the International Workshop on Age Determination of Oceanic Pelagic Fishes: Tunas, Billfishes, and Sharks (eds. E. D. Prince and L. M. Pulos). *NOAA Technical Report NMFS 8*. NOAA/NMFS, Silver Spring, MD, pp. 179–199.
- Campana, S.E. (2016). Transboundary movements, unmonitored fishing mortality, and ineffective international fisheries management pose risks for pelagic sharks in the Northwest Atlantic. *Canadian Journal of Fisheries and Aquatic Sciences*, 73, 1599-1607. <https://doi.org/10.1139/cjfas-2015-0502>
- Carney, R.S., (2005). Zonation of deep biota on continental margins. *Oceanogr. Mar. Biol.* 43, 211–278.
- Castro, J. A. and Mejuto, J. (1995) Reproductive parameters of blue shark, *Prionace glauca*, and other sharks in the Gulf of Guinea. *Marine and Freshwater Research* 46, 967–973
- Chan, F., Barth, J.A., Lubchenco, J., Kirincich, A., Weeks, H., Peterson, W.T., & Menge, B.A. (2008). Emergence of anoxia in the California Current large marine ecosystem. *Science*, 319, 920-920. <https://doi.org/10.1126/science.1149016>
- Chapman, L., Galis, F., Shinn, J., (2000). Phenotypic plasticity and the possible role of genetic assimilation: hypoxia induced tradeoffs in the morphological traits of an African cichlid. *Ecol. Lett.* 3, 387–393.
- Chavez FP, Messi'e M, Pennington JT. (2011). Marine primary production in relation to climate variability and change. *Annu. Rev. Mar. Sci.* 3:227–60
- Childress JJ, Seibel BA. (1998). Life at stable low oxygen levels: adaptations of animals to oceanic oxygen minimum layers. *J. Exp. Biol.* 201:1223–32
- Childress JJ. (1995). Are there physiological and biochemical adaptations of metabolism in deep-sea animals? *Trends. Ecol. Evol.* 10:30–36
- Clarke MR, Stevens JD (1974). Cephalopods, blue sharks and migration. *J Mar Biol Assoc UK* 54:949–957
- Coffey, D. M., Carlisle, A. B., Hazen, E. L., & Block, B. A. (2017). Oceanographic drivers of the vertical distribution of a highly migratory, endothermic shark. *Scientific Reports*, 7(1), 1–14. <https://doi.org/10.1038/s41598-017-11059-6>
- Davis, J.C., (1975). Minimal dissolved oxygen requirements of aquatic life with emphasis on Canadian species: a review. *J. Fish. Res. Bd. Can.* 32 (12), 2295–2332.
- Deutsch, C., Brix, H., Ito, T., & Thompson, L. (2011). Climate-Forced Variability of Ocean Hypoxia. *Science*, 333(July), 336–339. <https://doi.org/10.1126/science.1202422>
- Deutsch, C., Ferrel, A., Seibel, B., Portner, H.O., Huey, R.B., (2015). Climate change tightens a metabolic constraint on marine habitats. *Science* 348, 1132–1136.

- Diaz RJ, Rosenberg R (2008) Spreading dead zones and consequences for marine ecosystems. *Science* 321:926–929.
- Diaz RJ, Rosenberg R. (1995). Marine benthic hypoxia: a review of its ecological effects and the behavioural responses of benthic macrofauna. *Oceanogr. Mar. Biol. Annu. Rev.* 33:245–303
- Doney SC, Ruckelshaus M, Duffy JE, Barry JP, Chan F (2012). Climate change impacts on marine ecosystems. *Annu. Rev. Mar. Sci.* 4:11–37
- Drazen JC, Seibel BA. (2007). Depth-related trends in metabolism of benthic and benthopelagic deep-sea fishes. *Limnol. Oceanogr.* 52:2306–16
- Duffy, C. and Francis, M. P. (2001) Evidence of summer parturition in shortfin mako (*Isurus oxyrinchus*) sharks from New Zealand waters. *New Zealand Journal of Marine and Freshwater Research* 35, 319–324.
- Dulvy, N. K., J. K. Baum, S. Clarke, L. V. J. Compagno, E. Cortés, A. Domingo, S. Fordham, S. Fowler, M. P. Francis, C. Gibson, J. Martínez, J. A. Musick, A. Soldo, J. D. Stevens, and S. Valenti. (2008). You can swim but you can't hide: the global status and conservation of oceanic pelagic sharks. *Aquat. Cons. Mar. Freshw. Ecosys.* 18:459–482.
- Ekau W, Verheye HM. 2005. Influence of oceanographic fronts and low oxygen on the distribution of ichthyoplankton in the Benguela and southern Angola currents. *Afr. J. Mar. Sci.* 27:629–39
- Ekau, W., Auel, H., Portner, H. O., & Gilbert, D. (2010). Impacts of hypoxia on the structure and processes in pelagic communities (zooplankton, macro-invertebrates and fish). *Biogeosciences*, 7(5), 1669–1699. <https://doi.org/10.5194/bg-7-1669-2010>
- Farrell, A., Richards, J., (2009). Defining hypoxia: an integrative synthesis of the responses of fish to hypoxia. *Fish Physiol.* 27, 487–503.
- Ferretti F, Myers RA, Serena F, Lotze HK (2008) Loss of large predatory sharks from the Mediterranean Sea. *Conserv Biol* 22: 952–964.
- Ferretti, F., Worm, B., Britten, G. L., Heithaus, M. R., & Lotze, H. K. (2010). Patterns and ecosystem consequences of shark declines in the ocean. *Ecology Letters*, 13(8), 1055–1071. <https://doi.org/10.1111/j.1461-0248.2010.01489.x>
- Francis, M. P. and Duffy, C. (2005) Length at maturity in three pelagic sharks (*Lamna nasus*, *Isurus oxyrinchus*, and *Prionace glauca*) from New Zealand. *Fishery Bulletin* 103, 489–500.
- Friedman, J.R., Condon, N.E., Drazen, J.C., (2012). Gill surface area and metabolic enzyme activities of demersal fishes associated with the oxygen minimum zone off California. *Limnol. Oceanogr.* 57 (6), 1701–1710.
- Fuenzalida R, Schneider W, Garc'es Vargas J, Bravo L, Lange C. (2009). Vertical and horizontal extension of the oxygen minimum zone in the eastern South Pacific Ocean. *DeepSea Res. II* 56:992–1003
- Gallo, N. D., & Levin, L. A. (2016). Fish Ecology and Evolution in the World's Oxygen Minimum Zones and Implications of Ocean Deoxygenation. In *Advances in Marine Biology* (1st ed., Vol. 74). Elsevier Ltd. <https://doi.org/10.1016/bs.amb.2016.04.001>
- Gilly WF, Zeidberg LD, Booth JAT, Stewart JS, Marshall G, (2012). Locomotion and behavior of Humboldt squid, *Dosidicus gigas*, in relation to natural hypoxia in the Gulf of California, Mexico. *J. Exp. Biol.* 215:3175–90
- Gilly, W.F., Beman, J.M., Litvin, S.Y., & Robison, B.H. (2013). Oceanographic and biological effects of shoaling of the oxygen minimum zone. *Annual Review of*

- Marine Science, 5, 393-420. <https://doi.org/10.1146/annurev-marine-120710-100849>
- Gonzalez-Quiros R, Cabal J, Ivarez-Marques F, Isla A (2003) Ichthyoplankton distribution and plankton production related to the shelf break front at the Aviles Canyon. *ICES J Mar Sci* 60: 198–210.
- Grantham, B.A., Chan, F., Nielsen, K.J., Fox, D.S., Barth, J.A., Huyer, A., Lubchenko, J., Menge, B.A., (2004). Upwelling driven nearshore hypoxia signals ecosystem and oceanographic changes in the northeast Pacific. *Nature* 429, 749–754.
- Gray, J.S., Wu, R.S.S., Or, Y.Y., (2002). Effects of hypoxia and organic enrichment on the coastal marine environment. *Mar. Ecol. Prog. Ser.* 238, 249–279.
- Gregg WW, Casey NW, McClain CR. (2005). Recent trends in global ocean chlorophyll. *Geophys. Res. Lett.* 32:L03606
- Gruss A, Kaplan DM, Guenette S, Roberts CM, Botsford LW (2011) Consequences of adult and juvenile movements for marine protected areas. *Biol Conserv* 144: 692–702.
- Helly, J.J. and Levin, L.A. (2004). Global distribution of naturally occurring marine hypoxia on continental margins. *Deep Sea Res. I*, 51:1159–1168.
- Heupel MR, Carlson JK, Simpfendorfer CA (2007) Shark nursery areas: concepts, definition, characterization and assumptions. *Mar Ecol Prog Ser* 337: 287–297.
- Hochachka, P.W., Buck, L.T., Doll, C.J., Land, S.C., (1996). Unifying theory of hypoxia tolerance: molecular/metabolic defense and rescue mechanisms for surviving oxygen lack. *PNAS* 93, 9493–9498.
- Hofmann, A.F., Peltzer, E.T., Walz, P.M., Brewer, P.G., (2011). Hypoxia by degrees: establishing definitions for a changing ocean. *DeepSea Res. I* 58, 1212–1226.
- Holts, D. B. and Bedford, D. W. (1993) Horizontal and vertical movements of the Shortfin Mako shark, *Isurus oxyrinchus*, in the southern California Bight. *Australian Journal of Marine and Freshwater Research* 44, 901–909.
- Howey, L. A., Wetherbee, B. M., Tolentino, E. R., & Shivji, M. S. (2017). Biogeophysical and physiological processes drive movement patterns in a marine predator. *Movement Ecology*, 5(1), 16. <https://doi.org/10.1186/s40462-017-0107-z>
- International Commission for the Conservation of Atlantic Tunas (ICCAT). (2017a). Report of the 2017 ICCAT Shortfin Mako Stock Assessment meeting. Madrid, Spain. https://www.iccat.int/Documents/Meetings/Docs/2017_SMA_ASS_REP_ENG.pdf
- International Commission for the Conservation of Atlantic Tunas. 2019. Report of the Standing Committee on Research and Statistics (SCRS) (Madrid, Spain, 2019): ICCAT. https://www.iccat.int/Documents/Meetings/Docs/2019/REPORTS/2019_SCRS_ENG.pdf.
- IUCN (2009). IUCN Red list of threatened species. Version 2009. 2. <http://www.iucnredlist.org>
- IUCN. (2019). Ocean deoxygenation | IUCN. <https://www.iucn.org/resources/issues-briefs/ocean-deoxygenation>
- IUCN. (2019). Ocean deoxygenation | IUCN. <https://www.iucn.org/resources/issues-briefs/ocean-deoxygenation>
- Johnson DS, London JM, Lea MA, Durban JW. (2008). Continuous-time correlated random walk model for animal telemetry data. *Ecology* 89:1208–1215. DOI: <https://doi.org/10.1890/07-1032.1/PMID:18543615>

- Kamykowski, D., Zentara, S., (1990). Hypoxia in the world ocean as recorded in the historical data set. *Deep-Sea Res. I* 37, 1861–1874.
- Karstensen, J., Fiedler, B., Schütte, F., Brandt, P., Körtzinger, A., Fischer, G., Zantopp, R., Hahn, J., Visbeck, M., & Wallace, D. (2015). Open ocean dead zones in the tropical North Atlantic Ocean. *Biogeosciences*, 12(8), 2597–2605. <https://doi.org/10.5194/bg-12-2597-2015>
- Karstensen, Johannes, Stramma, L., & Visbeck, M. (2008). Oxygen minimum zones in the eastern tropical Atlantic and Pacific oceans. *Progress in Oceanography*, 77(4), 331–350. <https://doi.org/10.1016/j.pocean.2007.05.009>
- Keeling, R. F., Körtzinger, A., & Gruber, N. (2010). Ocean deoxygenation in a warming world. *Annual Review of Marine Science*, 2(1), 199–229. <https://doi.org/10.1146/annurev.marine.010908.163855>
- Key, R. M., Kozyr, A., Sabine, C. L., Lee, K., Wanninkhof, R., Bullister, J. L., Feely, R. A., Millero, F. J., Mordy, C., & Peng, T. (2004). A global ocean carbon climatology : Results from Global Data Analysis Project (GLODAP). *GLOBAL OCEAN CARBON CLIMATOLOGY*, 18, 1–23. <https://doi.org/10.1029/2004GB002247>
- Kroodsma, D. A., Mayorga, J., Hochberg, T., Miller, N. A., Boerder, K., Ferretti, F., Wilson, A., Bergman, B., White, T. D., Block, B. A., Woods, P., Sullivan, B., Costello, C., & Worm, B. (2018a). Response to Comment on “Tracking the global footprint of fisheries.” *Science*, 361(6404), 24–26. <https://doi.org/10.1126/science.aat6713>
- Kroodsma, D. A., Mayorga, J., Hochberg, T., Miller, N. A., Boerder, K., Ferretti, F., Wilson, A., Bergman, B., White, T. D., Block, B. A., Woods, P., Sullivan, B., Costello, C., & Worm, B. (2018b). Tracking the global footprint of fisheries. *Science (New York, N.Y.)*, 359(February), 904–908. <http://www.ncbi.nlm.nih.gov/pubmed/29472481>
- Kwiatkowski, L., Naar, J., Bopp, L., Aumont, O., Defrance, D., & Couespel, D. (2019). Decline in Atlantic Primary Production Accelerated by Greenland Ice Sheet Melt. *Geophysical Research Letters*, 46(20), 11347–11357. <https://doi.org/10.1029/2019GL085267>
- Lauvset, S. K., Lange, N., Tanhua, T., Bittig, H. C., Olsen, A., Kozyr, A., Álvarez, M., Becker, S., Brown, P. J., Carter, B. R., Cunha, L. C. da, Feely, R. A., Heuven, S. van, Hoppema, M., Ishii, M., Jeansson, E., Jutterström, S., Jones, S. D., Karlsen, M. K., ... Key, R. M. (2021). An updated version of the global interior ocean biogeochemical data product, GLODAPv2 . 2021. *Earth Syst. Sci. Data*, 13, 5565–5589. <https://doi.org/10.5194/essd-13-5565-2021>
- Levin LA. (2003b). Oxygen minimum zone benthos: adaptation and community response to hypoxia. *Oceanogr. Mar. Biol. Annu. Rev.* 41:1–45
- Levin, L. A. (2003a). Deep-Ocean life where oxygen is scarce. *The Scientific Research Society*, 90(5), 436–444. <https://doi.org/10.1511/2002.33.756>
- Luyten, J.R., Pedlosky, J., Stommel, H., 1983. The ventilated thermocline. *Journal of Physical Oceanography* 13, 292–309.
- Mandic, M., Ramon, M.L., Gracey, A.Y., Richards, J.G., 2014. Divergent transcriptional patterns are related to differences in hypoxia tolerance between the intertidal and the sub tidal sculpins. *Mol. Ecol.* 23, 6091–6103.
- Mandic, M., Todgham, A. E., & Richards, J. G. (2009). Mechanisms and evolution of hypoxia tolerance in fish. *Proceedings of the Royal Society B: Biological Sciences*, 276(1657), 735–744. <https://doi.org/10.1098/rspb.2008.1235>

- Marylou. B.E (2020a). *Blue Shark*. Azores Whale Watching TERRA AZUL™. <https://www.azoreswhalewatch.com/educational/speciescatalogue/elasmobranchs-and-teleosts/blue-shark/>
- Matey, V., Richards, J.G., Wang, Y., Wood, C.M., Rogers, J., Davies, R., Murray, B.W., Chen, X.Q., Du, J., Brauner, C.J., 2008. The effect of hypoxia on gill morphology and ionoregulatory status in the Lake Qinghai scaleless carp, *Gymnocypris przewalskii*. *J. Exp. Biol.* 211, 1063–1074.
- Matzinger, A., Schmid, M., Veljanoska-Sarafiloska, E., Patceva, S., Guseska, D., Wagner, B., Müller, B., Sturm, M., & Wüest, A. (2007). Thresholds of hypoxia for marine biodiversity. *Limnology and Oceanography*, 52(1), 338–353. <https://doi.org/10.4319/lo.2007.52.1.0338>
- Meissner, K.J., Galbraith, E.D., Völker, C., (2005). Denitrification under glacial and interglacial conditions: a physical approach. *Paleoceanography* 20, PA3001. <https://doi.org/10.1029/2004PA001083>
- Mentaschi, L., Besio, G., Cassola, F., & Mazzino, A. (2013a). Developing and validating a forecast/hindcast system for the Mediterranean Sea. *Journal of Coastal Research*, 65(SPEC. ISSUE 65), 1551–1556. <https://doi.org/10.2112/SI65-262.1>
- Mentaschi, L., Besio, G., Cassola, F., & Mazzino, A. (2013b). Problems in RMSE-based wave model validations. *Ocean Modelling*, 72, 53–58. <https://doi.org/10.1016/j.ocemod.2013.08.003>
- Miller, D., Poucher, S., & Coiro, L. (2002). Determination of lethal dissolved oxygen levels for selected marine and estuarine fishes, crustaceans, and a bivalve. *Marine Biology*, 140, 287–296. <https://doi.org/10.1007/s002270100702>
- Mucientes GR, Queiroz N, Sousa LL, Tarroso P, Sims DW (2009) Sexual segregation of pelagic sharks and the potential threat from fisheries. *Biol Lett* 5: 156–159.
- Nakano, H. and Seki, M. P. (2003). Synopsis of biological data on the blue shark *Prionace glauca* Linnaeus. *Bulletin of the Fisheries Research Agency* 6, 18–55.
- Nakano, H., & Stevens, J. D. (2009). The Biology and Ecology of the Blue Shark, *Prionace glauca*. *Sharks of the Open Ocean: Biology, Fisheries and Conservation*, 140–151. <https://doi.org/10.1002/9781444302516.ch12>
- Nasby-Lucas, N., Dewar, H., Lam, C. H., Goldman, K. J., & Domeier, M. L. (2009). White shark offshore habitat: A behavioral and environmental characterization of the eastern pacific shared offshore foraging area. *PLoS ONE*, 4(12). <https://doi.org/10.1371/journal.pone.0008163>
- Nasby-Lucas, N., Dewar, H., Sosa-Nishizaki, O., Wilson, C., Hyde, J. R., Vetter, R. D., Wraith, J., Block, B. A., Kinney, M. J., Sippel, T., Holts, D. B., & Kohin, S. (2019). Movements of electronically tagged Shortfin Mako sharks (*Isurus oxyrinchus*) in the eastern North Pacific Ocean. *Animal Biotelemetry*, 7(1), 1–26. <https://doi.org/10.1186/s40317-019-0174-6>
- Olsen, A., Lange, N., Key, R. M., Tanhua, T., Bittig, H. C., Kozyr, A., Álvarez, M., Azetsu-scott, K., Becker, S., Brown, P. J., Carter, B. R., Brown, P. J., Carter, B. R., Cunha, L. C. da, Feely, R. A., Heuven, S. van, Hoppema, M., Ishii, M., Jeansson, E., ... Woosley, R. J. (2020). An updated version of the global interior ocean biogeochemical data product , GLODAPv2.2020. *Earth Syst. Sci. Data*, 12(July), 3653–3678. <https://doi.org/10.5194/essd-12-3653-2020>
- Paerl HW (2006) Assessing and managing nutrient-enhanced eutrophication in estuarine and coastal waters: Interactive effects of human and climatic perturbations. *Ecological Engineering* 26:40–54
- Pasqualotto, N., D'Urso, G., Bolognesi, S. F., Belfiore, O. R., Van Wittenberghe, S., Delegido, J., Pezzola, A., Winschel, C., & Moreno, J. (2019). Retrieval of

- evapotranspiration from sentinel-2: Comparison of vegetation indices, semi-empirical models and SNAP biophysical processor approach. *Agronomy*, 9(10). <https://doi.org/10.3390/agronomy9100663>
- Patterson TA, Thomas L, Wilcox C, Ovaskainen O, Matthiopoulos J (2008) State-space models of individual animal movement. *Trends. Ecol Evol* 23: 87–94.
- Paulmier, A., & Ruiz-Pino, D. (2009). Oxygen minimum zones (OMZs) in the modern ocean. *Progress in Oceanography*, 80(3-4), 113–128. <https://doi.org/10.1016/j.pocean.2008.08.001>
- Payne NL, Smith JA, Meulen DE, Taylor MD, Watanabe YY, Takahashi A, Marzullo TA, Gray CA, Cadiou G, Suthers IM (2016) Temperature dependence of fish performance in the wild: links with species biogeography and physiological thermal tolerance. *Funct Ecol* 30: 903–912.
- Paytan, A., & McLaughlin, K. (2007). The oceanic phosphorus cycle. *Chemical Reviews*, 107, 563–576. <https://doi.org/10.1021/cr0503613/cr0503613>
- Penn, J. L., Deutsch, C., Payne, J. L., & Sperling, E. A. (2018). Temperature-dependent hypoxia explains biogeography and severity of end-Permian marine mass extinction. *Science*, 362(6419). <https://doi.org/10.1126/science.aat1327>
- Perruche, C., Szczypta, C., Paul, J., & Drévillon, M. (2019). Global Production Centre GLOBAL_REANALYSIS_BIO_001_029.
- Polovina JJ, Howell EA, Abecassis M. (2008). Ocean’s least productive waters are expanding. *Geophys. Res. Lett.* 35:L03618
- Portner HO, Farrell AP. (2008). Physiology and climate change. *Science* 322:690–92
- Prince, E. D. & Goodyear, C. (2006). Hypoxiased habitat compression of tropical pelagic fishes. *Fish. Oceanography*. 15, 451–464.
- Prince, E. D., Luo, J., Phillip Goodyear, C., Hoolihan, J. P., Snodgrass, D., Orbesen, E. S., Serafy, J. E., Ortiz, M., & Schirripa, M. J. (2010). Ocean scale hypoxia-based habitat compression of Atlantic istiophorid billfishes. *Fisheries Oceanography*, 19(6), 448–462. <https://doi.org/10.1111/j.1365-2419.2010.00556.x>
- Queiroz, N., Humphries, N. E., Couto, A., Vedor, M., da Costa, I., Sequeira, A. M. M., Mucientes, G., Santos, A. M., Abascal, F. J., Abercrombie, D. L., Abrantes, K., Acuña-Marrero, D., Afonso, A. S., Afonso, P., Anders, D., Araujo, G., Arauz, R., Bach, P., Barnett, A., ... Sims, D. W. (2019). Global spatial risk assessment of sharks under the footprint of fisheries. *Nature*, 572(7770), 461–466. <https://doi.org/10.1038/s41586-019-1444-4>
- Queiroz, N., Humphries, N. E., Mucientes, G., Hammerschlag, N., Lima, F. P., Scales, K. L., Miller, P. I., Sousa, L. L., Seabra, R., & Sims, D. W. (2016). Ocean-wide tracking of pelagic sharks reveals extent of overlap with longline fishing hotspots. *Proceedings of the National Academy of Sciences of the United States of America*, 113(6), 1582–1587. <https://doi.org/10.1073/pnas.1510090113>
- Queiroz, N., Humphries, N. E., Noble, L. R., Santos, A. M., & Sims, D. W. (2012). Spatial dynamics and expanded vertical niche of blue sharks in oceanographic fronts reveal habitat targets for conservation. *PLoS ONE*, 7(2). <https://doi.org/10.1371/journal.pone.0032374>
- Queiroz, N., Vila-Pouca, C., Couto, A., Southall, E. J., Mucientes, G., Humphries, N. E., & Sims, D. W. (2017). Convergent foraging tactics of marine predators with different feeding strategies across heterogeneous ocean environments. *Frontiers in Marine Science*, 4(AUG), 1–15. <https://doi.org/10.3389/fmars.2017.00239>

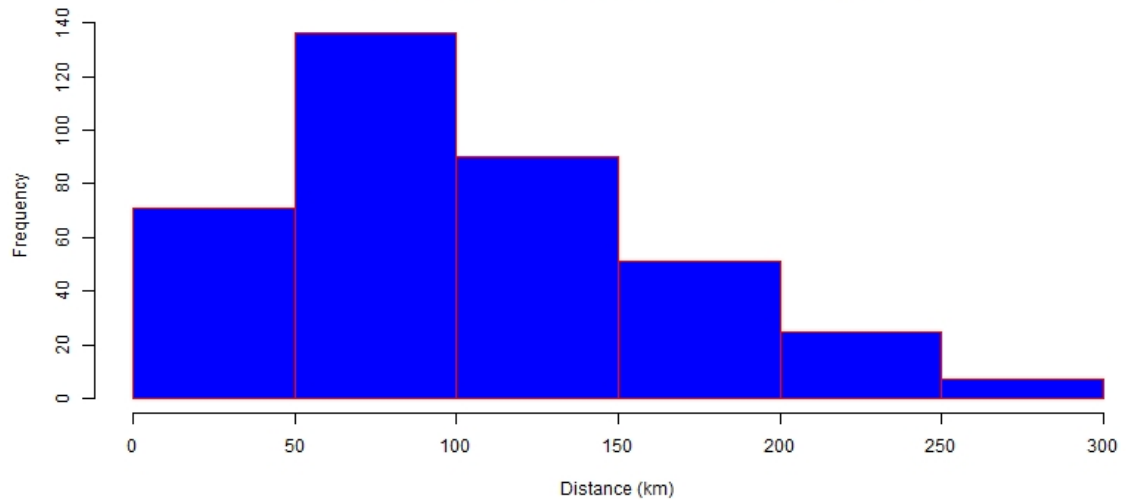
- Richards, J., 2009. Metabolic and molecular responses of fish to hypoxia. *Fish Physiol.* 27, 443–485.
- Roberts, J. L (1978). The Physiological Ecology of Tunas. *Nature* 7, 83–88
- Rogers, N. J., Urbina, M. A., Reardon, E. E., McKenzie, D. J., & Wilson, R. W. (2016). A new analysis of hypoxia tolerance in fishes using a database of critical oxygen level (Pcrit). *Conservation Physiology*, 4(1), 1–19. <https://doi.org/10.1093/conphys/cow012>
- Semenza, G.L., (1998). Hypoxia-inducible factor 1: master regulator of O₂ homeostasis. *Curr. Opin. Genet. Dev.* 8 (5), 588–594.
- Shepard, M.P., (1955). Resistance and tolerance of young speckled trout (*Salvelinus fontinalis*) to oxygen lack, with special reference to low oxygen acclimation. *J. Fish. Res. Board Can.* 12, 387–446.
- Sims D. W (2005). Differences in habitat selection and reproductive strategies of male and female sharks. In Ruckstuhl KE and Neuhaus P (Eds), Sexual Segregation in Vertebrates: Ecology of the Two Sexes. *Cambridge University Press*, Cambridge, UK, pp. 127–147.
- Sims, D. W., Humphries, N. E., Bradford, R. W., & Bruce, B. D. (2012). Lévy flight and Brownian search patterns of a free-ranging predator reflect different prey field characteristics. *Journal of Animal Ecology*, 81(2), 432–442. <https://doi.org/10.1111/j.1365-2656.2011.01914.x>
- Stevens, J. D. (2009). The Biology and Ecology of the Shortfin Mako shark, *Isurus oxyrinchus*. *Sharks of the Open Ocean: Biology, Fisheries and Conservation*, 87–94. <https://doi.org/10.1002/9781444302516.ch7>
- Stevens, J. D. and Wayte, S. S. (1999) A Review of Australia's Pelagic Shark Resources. Final Report, Project 89/107. Fisheries Research and Development Corporation, Deakin West, Australian Capital Territory, Australia, 64 pp.
- Stevens, J. D., Bradford, R. W., & West, G. J. (2010). Satellite tagging of blue sharks (*Prionace glauca*) and other pelagic sharks off eastern Australia: Depth behaviour, temperature experience and movements. *Marine Biology*, 157(3), 575–591. <https://doi.org/10.1007/s00227-009-1343-6>
- Stramma L, Oschlies A, Schmidtko S. (2012). Anticorrelated observed and modeled trends in dissolved oceanic oxygen over the last 50 years. *Biogeosci. Discuss.* 9:4595–626
- Stramma L, Prince ED, Schmidtko S, Luo J, Hoolihan JP, (2011). Expansion of oxygen minimum zones may reduce available habitat for tropical pelagic fishes. *Nat. Clim. Change* 2:33–37
- Stramma L, Schmidtko S, Levin LA, Johnson GC. (2010). Ocean oxygen minima expansions and their biological impacts. *DeepSea Res. I* 57:587–95
- Stramma L., J. Fischer, P. Brandt, F. Schott, (2003). In *Interhemispheric Water Exchange in the Atlantic Ocean*, G. J. Goni, P. Malanotte Rizzoli, Eds., pp. 1–22.
- Stramma, L., Johnson, G. C., Sprintall, J., & Mohrholz, V. (2008). Expanding oxygen-minimum zones in the tropical oceans. *Science*, 320(5876), 655–658. <https://doi.org/10.1126/science.1153847>
- Stramma, L., Prince, E. D., Schmidtko, S., Luo, J., Hoolihan, J. P., Visbeck, M., Wallace, D. W. R., Brandt, P., & Körtzinger, A. (2012). Expansion of oxygen minimum zones may reduce available habitat for tropical pelagic fishes. *Nature Climate Change*, 2(1), 33–37. <https://doi.org/10.1038/nclimate1304>

- U.S. Environmental Protection Agency (2000) Ambient Aquatic Life Water Quality Criteria for Dissolved Oxygen (Saltwater): Cape Cod to Cape Hatteras (*EPA Publication 822R00-012*) (EPA, Washington, DC)
- Vedor, M., Queiroz, N., Mucientes, G., Couto, A., da Costa, I., Dos Santos, A., Vandeperre, F., Fontes, J., Afonso, P., Rosa, R., Humphries, N. E., & Sims, D. W. (2021). Climate-driven deoxygenation elevates fishing vulnerability for the ocean's widest ranging shark. *ELife*, *10*, 1–29. <https://doi.org/10.7554/eLife.62508>
- Vetter R, Kohin S, Preti A. 2008. Predatory interactions and niche overlap between Mako shark, *Isurus oxyrinchus*, and jumbo squid, *Dosidicus gigas*, in the California Current. *CalCOFI Rep.* *49*:142–56
- Walli, A., Teo, S. L. H., Boustany, A., Farwell, C. J., Williams, T., Dewar, H., Prince, E., & Block, B. A. (2009). Seasonal movements, aggregations and diving behavior of Atlantic bluefin tuna (*Thunnus thynnus*) revealed with archival tags. *PLoS ONE*, *4*(7). <https://doi.org/10.1371/journal.pone.0006151>
- Ward P, Myers RA (2005) Shifts in Open-Ocean Fish Communities Coinciding With the Commencement of Commercial Fishing. *Ecology* *86*: 835–847.
- Weng KC, Boustany AM, Pyle P, Anderson SD, Brown A, Block BA (2007) Migration and habitat of white sharks (*Carcharodon carcharias*) in the eastern Pacific Ocean. *Mar Biol* *152*:877–894
- Weng KC, Castilho PC, Morrissette JM, Landeira-Fernandez AM and others (2005) Satellite tagging and cardiac physiology reveal niche expansion in salmon sharks. *Science* *310*:104–106
- Whitney FA, Freeland HJ, Robert M. (2007). Persistently declining oxygen levels in the interior waters of the eastern subarctic Pacific. *Prog. Oceanogr.* *75*:179–99
- Williams, F. (1977) Notes on the biology and ecology of the blue shark (*Prionace glauca* L.) in the eastern Pacific Ocean and a review of data from the world ocean. Unpublished report, 16 pp
- Wohlers J, Engel A, Zöllner E, Breithaupt P, Jürgens K, et al. (2009). Changes in biogenic carbon flow in response to sea surface warming. *Proc. Natl. Acad. Sci. USA* *106*:7067–72
- Wood AG, Naef-Daenzer B, Prince PA, Croxall JP (2000) Quantifying habitat use in satellite-tracked pelagic seabirds: application of kernel estimation to albatross locations. *Journal of Avian Biology* *31*: 278–286
- Worm, B., Davis, B., Kettner, L., WardPaige, C.A., Chapman, D., Heithaus, M.R., ... Gruber, S.H. (2013). Global catches, exploitation rates, and rebuilding options for sharks. *Marine Policy*, *40*, 194204. <https://doi.org/10.1016/j.marpol.2012.12.034>
- Wright JJ, Konwar KM, Hallam SJ. (2012). Microbial ecology of expanding oxygen minimum zones. *Nat. Rev. Microbiol.* *10*:381–94

Appendix

Appendix 1

Distance variation between Blue Shark and GLODAP Fields



Distance variation between Mako Shark and GLODAP Fields

